ANODE SHAPE PREDICTION IN ELECTROCHEMICAL MACHINING WITH COMPOSITE PROGRAMME CONTROLLED TOOL

By

DEVASHISH BANERJI

Th
ME|1985|M
B 223a

DEPARTMENT OF MECHANICAL ENGINEERING

DIAN INSTITUTE OF TECHNOLOGY, KANPUR

APRIL, 1985

ANODE SHAPE PREDICTION IN ELECTROCHEMICAL MACHINING WITH COMPOSITE PROGRAMME CONTROLLED TOOL

A Thesis Submitted
In Partial Fulfilment of the Requirements
for the Degree of

MASTER OF TECHNOLOGY

By
DEVASHISH BANERJI

to the

DEPARTMENT OF MECHANICAL ENGINEERING
INDIAN INSTITUTE OF TECHNOLOGY, KANPUR
APRIL, 1985

12 JUN 1985

I.I.T KANPUR
CENTRAL LIBRARY

Thesis
621.93
B223a

ME-1985-M-BAN-ANO

CERTIFICATE

This is to certify that the work entitled, "Anode Shape Prediction in Electrochemical Machining with Composite Programme Controlled Tool" by Devashish Banerji has been carried out under my supervision and has not been submitted elsewhere for a degree.

April, 1985

Dr. A. Ghosh
Professor
Dept. of Mechanical Engg.
Indian Institute of Tech.
Kanpur-208016

115075

ACKNOWLEDGEMENTS

With profound sense of gratitude, I wish to put on record my sincere thanks to Dr. Amitabha Ghosh, who has guided this work from conception to completion.

I would like to thank Mr. V. Raghuram for his valuable suggestions and constant help during the course of work.

I am thankful to my friends Messers G.N.M. Sudhakar, M. Oza, I.K. Bhat, Dinesh Kumar, Alok Shrivastava and H. Markale for their valuable co-operation and timely help provided whenever necessary.

I also express my appreciation to Mr. Bhartiya for rendering his services in fabricating the experimental set-up.

Finally, I am thankful to Mr. D.P. Saini and Mr. B.K. Jain for producing the work in the present form.

DEVASHISH BANERJI

CONTENTS

LIST OF FIGURES

NOMENCLATURE

A	-	atomic weight of anode material in gm.
a	-	side of a square mesth.
C	-	the capacitance, μF.
F	-	Faraday's constant, 96500 Coulombs.
h	-	step height
i,j,k	-	coordinates of any arbitrary point.
J	-	current density Amp/cm^2.
k	-	conductivity of the electrolyte mho/cm
r, z	-	cylindrical coordinatez.
R	-	the electrical resistance, ohm
T_1, T_2, T_3	-	duty cycle of machining for Section 1, 2 and 3.
V	-	voltage applied to the anode.
z	-	valence of dissolution
ø	-	potential
ρ_w	-	density of the anode, g/cm^3

ABSTRACT

Recently, the new concept of using composite programme controlled ECM tool to produce different work-shapes, has been proposed (1). In the present work theoretical analyses have been conducted to predict the anode shapes generated by the composite ECM tool, with controlled duty cycle. A computational algorithm for each of the following two tools has been developed.

1. An annular composite tool.
2. A square composite tool having a matrix of square elements.

An experimental work involving the annular composite tool has been conducted to study the feasibility of the procedure. It is found that the work-geometries obtained depend on the duty cycles of the various sections - of the composite tool and the concept of using composite programme controlled ECM tool is practicable.

CHAPTER-1

INTRODUCTION

Electrochemical machining was initially introduced to machine those alloys, which are high strength and heat resistant materials. This process found its genesis in the electrolysis process, whose laws were established by Faraday in 1833. In electrochemical machining, the process of electrolytic dissolution takes place at the anode (workpiece). A suitably shaped cathode forms the tool. The tool and the workpiece are kept separated by a very small distance, filled with flowing electrolyte. A high current is required to affect the material removal at a reasonable rate.

ECM process can often be used to produce complex shapes by suitably shaping the cathode (tool). As mentioned earlier, due to the absence of any of the mechanical forces, this process offers excellent opportunity to machine hard and tough materials. ECM has also been known to produce a stress free surface. This process has found popularity in the Aerospace and many other modern industries and it is generally used for cavity

sinking, drilling, trepanning, sawing, cutting off and honing.

Anodic shaping under the known machining conditions is one of the fundamental problems which confronts the researchers. But the actual problem, i.e. the determination of a required tool shape for producing a prescribed workgeometry, is a more difficult problem. The lack of progress in solving this problem has resulted in empirical and other cut and try methods.

McGeough et al.,(2) suggested a perturbation technique to describe the electrochemical shaping when the amplitude of shapes on the cathode and the anode are small compared to the interelectrode gap. Though this method also solves the overpotential problem, it is restricted by the small size it can handle. Another method which was suggested by Collet et al.,(3) is based on the solution to the Laplace's equation by complex variable method. But the theoretical results are not always in good agreement with the experimental results. This may be due to the fact that the effects of the flow of electrolyte and the overpotential are not taken into consideration. Tusuei and Tipton (4) have given the " cos θ" method which can be used yielding good results for gentle shapes. The cos θ method can be applied where

the electric field can be assumed to be normal to the surfaces of electrodes. Hewson and Brown (5) extended the work of Collet et al., and employed the method of conformal mapping for the analysis of the two dimensional problems. Jain and Pandey (6) have worked on the application of Finite Element Technique to design analysis of ECM tools. The results obtained have a good correlation with the experimental results. The recent works have shown that the best results seem to be offered by the numerical methods.

1.1 PRESENT WORK:

From the above literature it is apparent that the earlier theoretical models involve a tedious trial and error process to determine the final tool shape. Moreover, different tools are required to generate different shapes. It has been recently suggested (1, 7, and 8) that a single composite programme-controlled (CPC) ECM tool may produce different workshapes by controlling the tool surface potential. The objective of the present work is to study the various shapes produced by such a tool with prescribed cathode potential control. The tool surface is given uniform potential. But the variations in the workgeometry are achieved by controlling the duty cycle of each section independently.

A theoretical analysis has been developed by devising a computational algorithm for predicting the metal removal rate and worksurface produced under the following conditions·

(1) A suitable potential is applied to the three annular sections of a cylindrical composite tool for different intervals of time.

(2) A suitable potential is applied for different intervals of time to the elements of a square composite tool having a matrix of square elements insulated for each other.

Some simple experiments were also conducted for the annular composite tool. The objective of these experiments were to study the feasibility of the theoretical work.

However, this is a preliminary attempt to investigate into different aspects of this suggested new approach. A meaningful hardware implementation of suggested idea will require quite elaborate facilities and significant funds. Thus, it is beyond the scope of the present thesis.

CHAPTER-2

THEORETICAL ANALYSIS

2.1 INTRODUCTION:

Electrochemical machining utilizes a tool (cathode) kept at a uniform potential with respect to the workpiece (anode). When this is a formed tool, a complementary surface is supposed to be cut on the workpiece through electrolytic dissolution. But there are some limitations in using a formed tool, foremost being that a single tool produces only one work-geometry.

A theoretical analysis has been presented in this section for the plane composite cathodes. Each section of the CPC tool is given voltage for different time interval. The composite tools which have been considered are as follows:

(1) An axisymmetric cylindrical composite tool with annular sections (Fig. 2.11).

(2) An eight by eight matrix of square and identical elements (Fig. 2.12).

The above concept of the composite tools using different duty cycle for each section to machine a formed

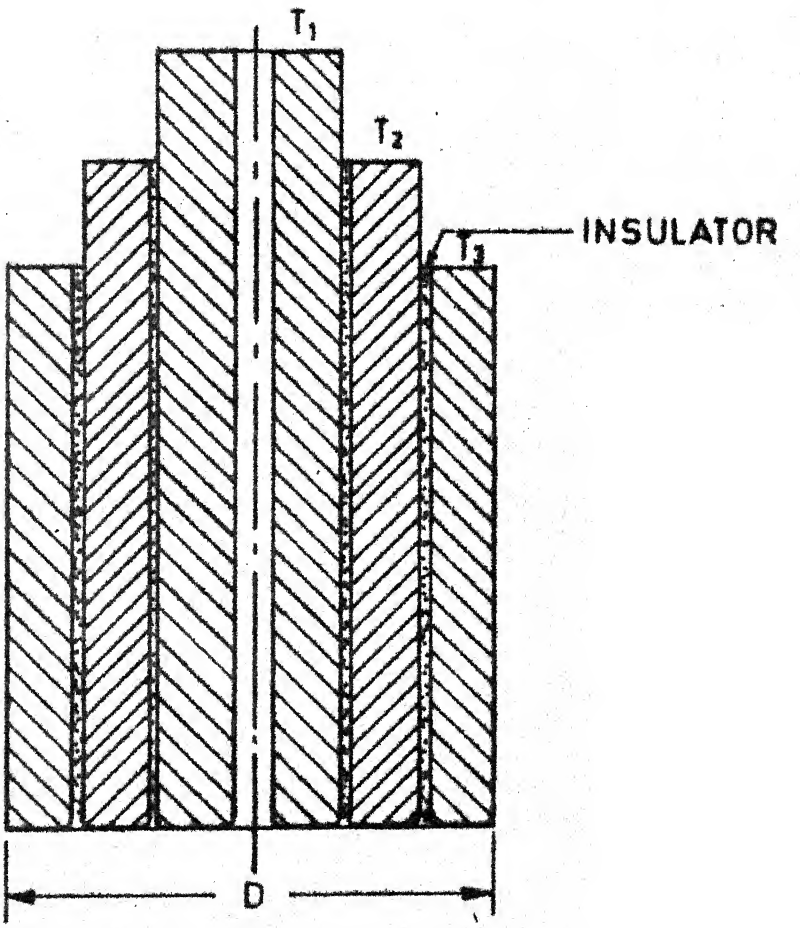

Fig. 2.11 Annular Tool

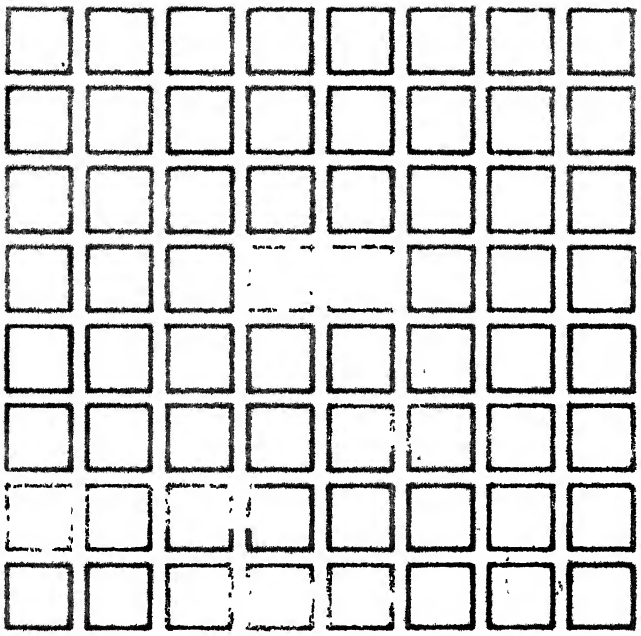

Fig. 2.12 Square composit tool

surface can be explained by a simple example (Fig. 2.13). The tool comprises of two sections A and B. They are properly insulated from each other by a thin lamina. The workpiece(anode) is kept at a uniform potential with respect to both the sections. But on-time for both the sections vary. If it were T_1 for A and T_2 for B and $T_2 > T_1$ then greater amount of machining will take place under the section B. The worksurface produced will be as shown in Fig. 2.13. By controlling the duty cycle in each section, the step height can be varied.

2.2 CASE 1: ANNULAR COMPOSITE TOOL:

As mentioned earlier, this work is concerned with the prediction of the worksurface produced by the composite tools. The analysis for the cylindrical tool which generates axisymmetric surfaces follows first.

In order to theoretically predict the workshapes generated by the composite tool, first it is necessary to obtain the potential distribution across the electrodes. The potential distribution across the electrode gap can be obtained by solving the Laplaces equation (2.22) for given boundary conditions.

The Laplaces equation has been solved by using the finite difference method. A Fortran programme has been developed to complete the iterations involved. The

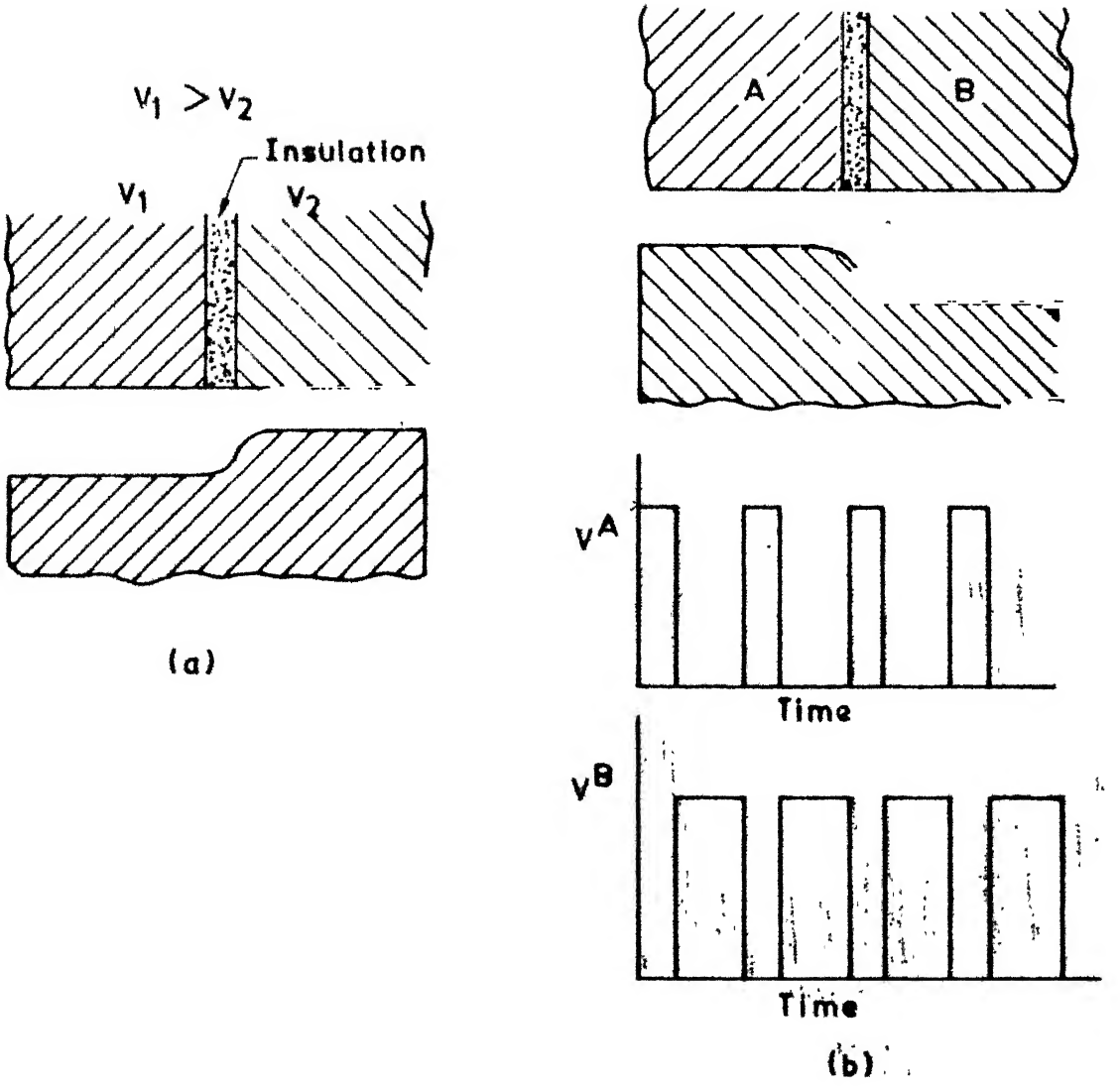

Fig. 2.13 Principle of Composite ECM Tool.

change in the configuration of the worksurface is obtained from the Faraday's law. The iterations are repeated till the configuration reaches a steady state*.

In electrochemical machining, the dissolution of the anode (r_w) for a small time interval is given by:

$$\dot{r}_w = \frac{J\,A}{Z\,F\,\rho_w} \qquad 2.21$$

where

J = current density in amps/cm^2 (-kg rad ϕ).

A = the atomic weight in grams.

Z = the valence of dissolution.

ρ_w = the density in g/cc of anode material.

k = the conductivity of electrolyte in mho/cm.

ϕ = potential in volts.

F = the Faraday's constant.

To find out grad ϕ, the evaluation of the potential distribution is required. Numerical solution to this problem requires specification of the coordinates of both the cathode and the anode. These coordinates can be defined in terms of an equispaced rectangular mesh (Fig. 2.21). The grid points of this mesh are defined by the coordinates (i, j) (Fig. 2.21). A suitable scale, in terms of the mesh spacing is chosen for the cathode and the

---

* However, it should be noted that a steady state can not be obtained when no feed is given to the tool.

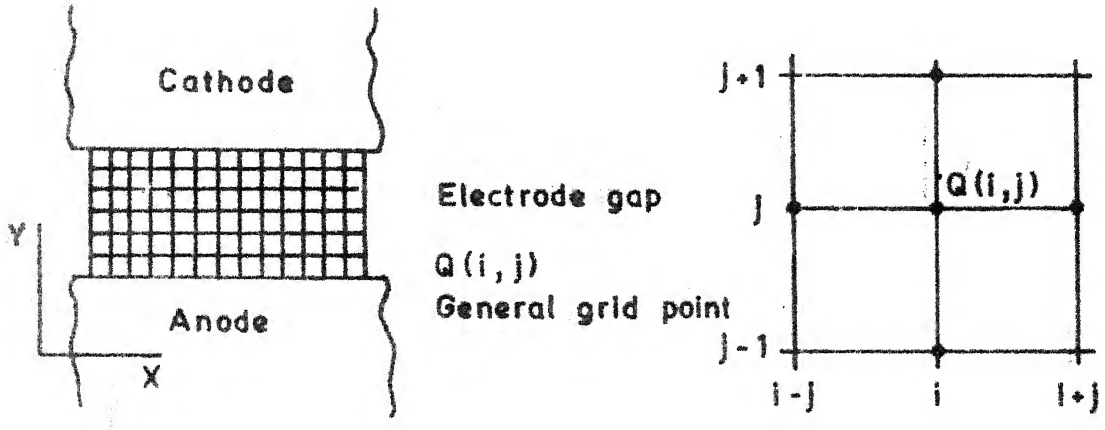

(a)

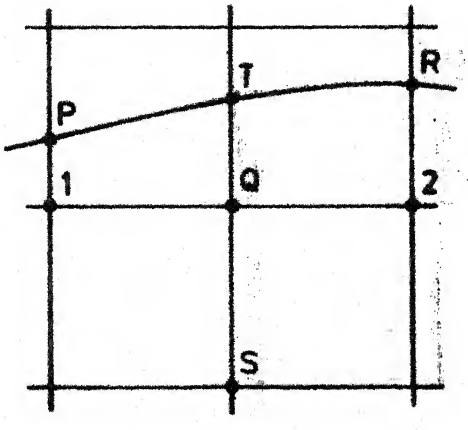

(b)

Fig. 2.21 (a) Development of Finite Difference Method with a point Q (i, j)

(b) Section of the Electrode Boundary, PTR

anode shapes. The potential field in the space between the electrodes can be evaluated by solving the Laplace's equation (2.22) for the specified boundary conditions.

The Laplace's equation for the axisymmetric case (when the tool is cylindrical in shape, Fig. 2.11 can be written as;

$$\frac{\partial^2 \phi}{\partial r^2} + \frac{1}{r}\frac{\partial \phi}{\partial r} + \frac{\partial^2 \phi}{\partial z^2} = 0 \qquad 2.22$$

where ϕ is the potential and r, z are the cylindrical coordinates.

The simplified form of the equation (2.22) in the finite difference form can be expressed as follows:

$$[\phi(i,j+1) + \phi(i,j-1) + \phi(i+1,j) + \phi(i+1,j)(1+1/2i) + \phi(i-1,j)(1 - \frac{1}{2i})] / 4 = \phi(i,j) \qquad 2.23$$

Here $\phi(i,j)$ is the value of the potential on any grid point (i,j).

The details of the derivation of this equation is given in Appendix (A). It is obvious that if the potential at the four neighbouring points are known, then the potential at a point can be estimated.

The boundary conditions in this case are specified as follows:

(1) The potential at the grid points on the cathode surface is fixed as 0 volts.

(2) The potential at the grid points on the anode boundary is fixed at some suitable value V_o (10 V for the present case).

(3) $dv/dr = 0$, at $r = 0$ and $r = R$, this condition is satisfied by using the mirror symmetry. Thereby setting the values of potentials at the grid points on the sides of AB and EF of the rectangular mesh Fig. 2.22.

(4) $dv/dy' = 0$ in the segment which is not connected at that particular time interval.

An initial value of ϕ is assumed for the grid points, excluding the grid points on the anode and the cathode. Using the above boundary conditions and initial values, the following equation is made to satisfy.

$$\phi(i,j+1) + \phi(i,j-1) + \phi(i+1,j)(1+1/2i) + \phi(i-1,j)(1 - 1/2i) - 4\phi(i,j) = R \qquad 2.24$$

Here R is the value by which the left hand side of the equation (2.23) differs from zero. The maximum value of R gives the measure of the deviation of the solution from the correct solution. The required solution is obtained by minimizing the value of R in each iteration.

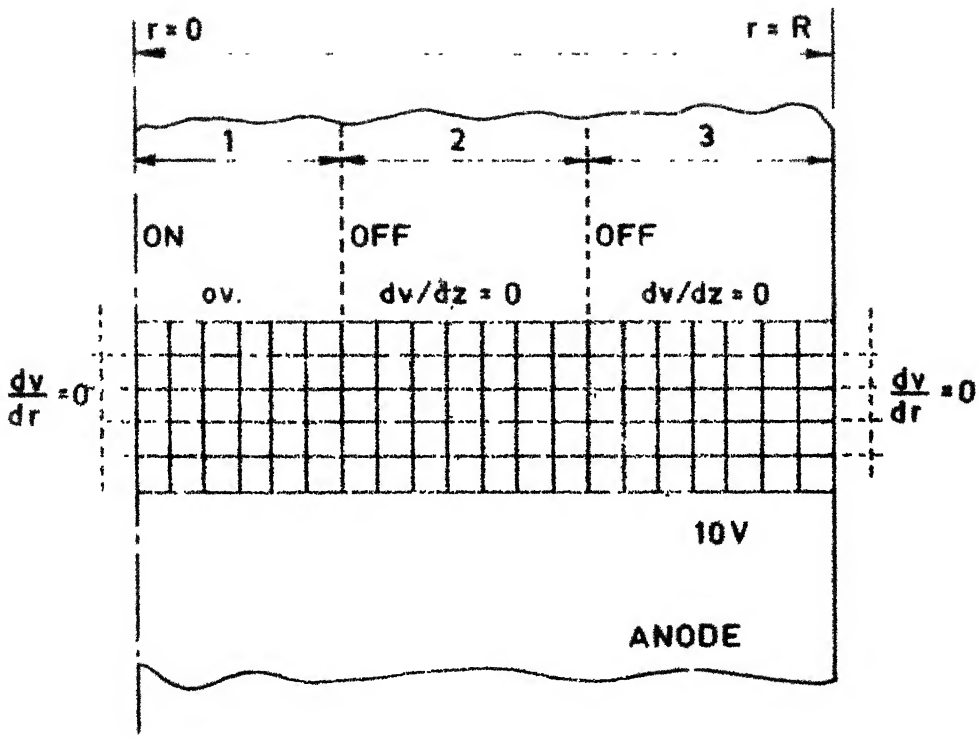

Fig. 2.22 Boundary Conditions for Axicymmetric case.

Once the potential distribution across the electrodes is known, the amount of metal dissolution can be obtained by using equation (2.21). A new anode boundary emerges after each cycle. Then, the equipotential boundary of the anode may intersect the vertical lines of the mesh at the points P, T and R as shown in Fig. 2.21. It can be seen that these points are not the regular grid points, and the above finite difference equation can not be directly employed. The potential at Q is found by linear interpolation using the values at S and T. The potential at the other points are found by using equation (2.21).

The amount of the dissolution of the anode material is computed for a finite time interval . Then the anode boundary is moved by a distance determined by the distribution of the material dissolved. The cathode surface is also moved as a rigid body by an amount specified by the feed. The same procedure is repeated till the change in the anode shape becomes negligible.

All the above steps, which are necessary to compute the material removal rate and the anode boundary, have been incorporated in a programme using Fortran-IV. The flow charts, illustrating the programme are as shown in the Figs. 2.23, 2.24 and 2.25.

MAIN PROGRAMME

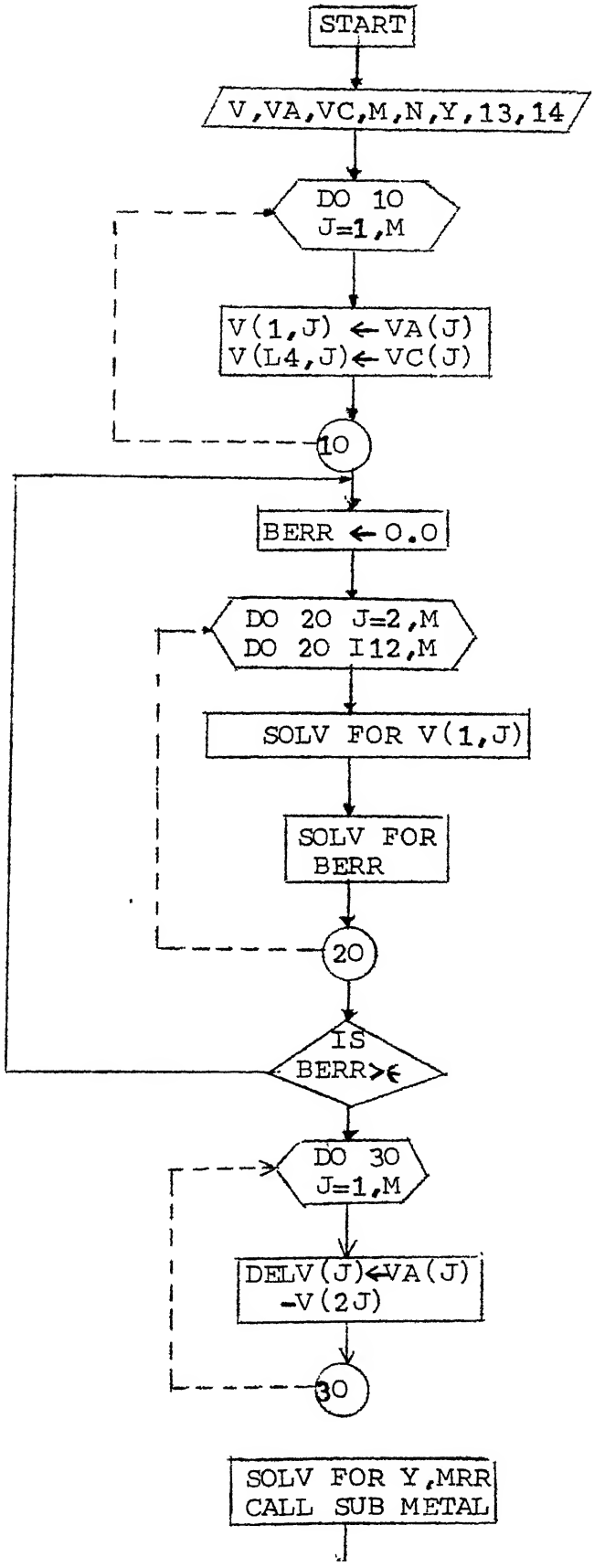

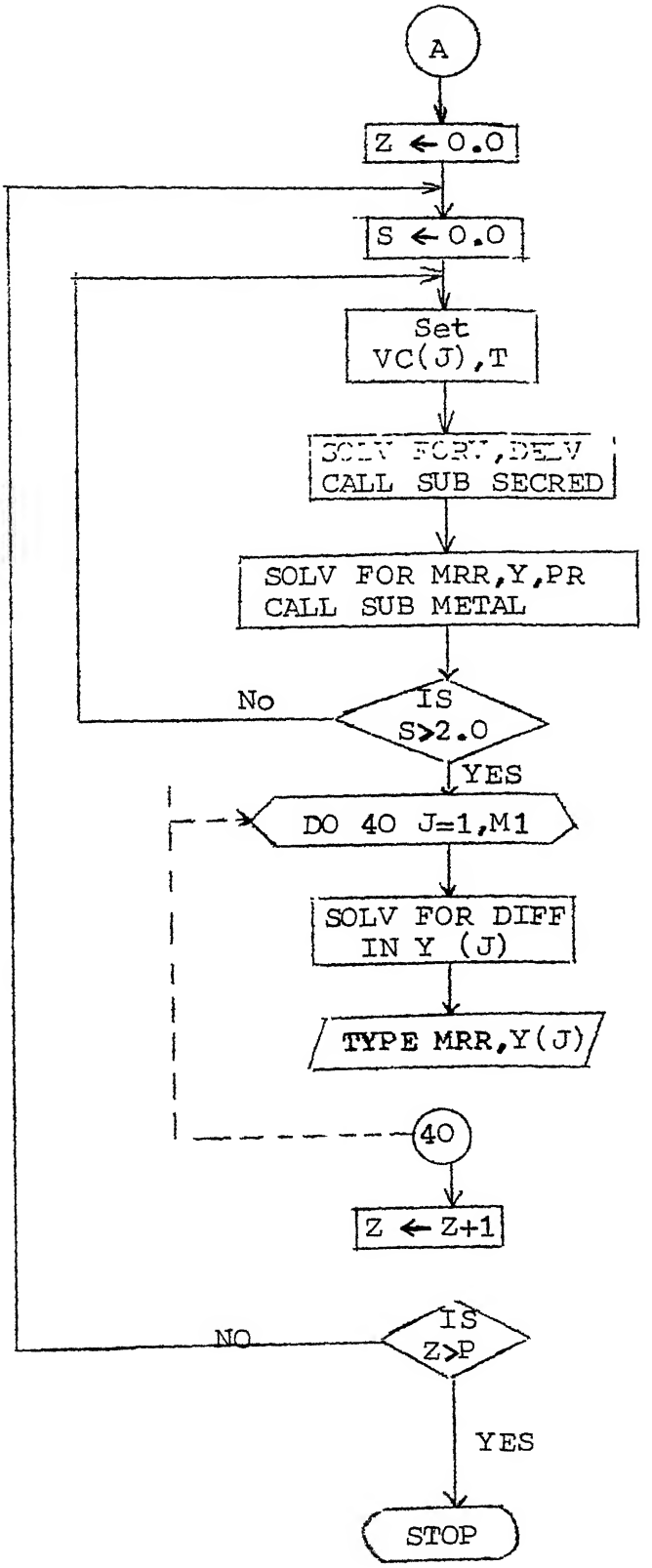
A
Z ← 0.0
S ← 0.0
Set
VC(J),T
SOLV FOR Y,DELV
CALL SUB SECRED
SOLV FOR MRR,Y,PR
CALL SUB METAL
No
IS
S>2.0
YES
DO 40 J=1,M1
SOLV FOR DIFF
IN Y (J)
TYPE MRR,Y(J)
40
Z ← Z+1
NO
IS
Z>P
YES
STOP

FIG. 2.23

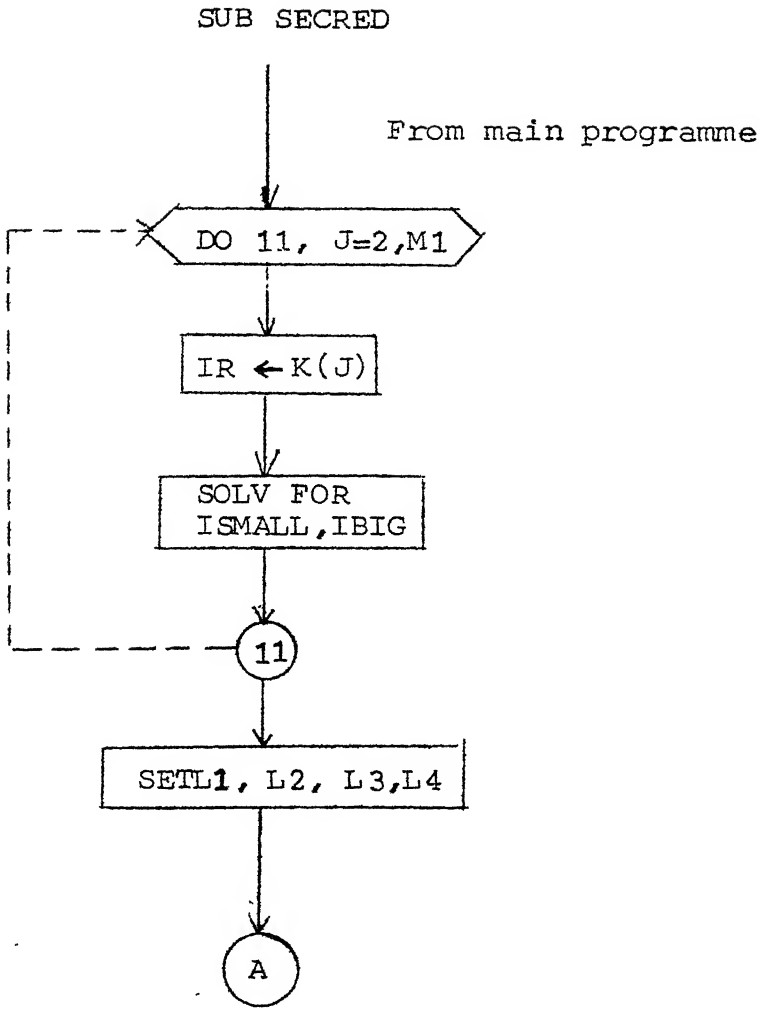
SUB SECRED
From main programme
DO 11, J=2,M1
IR ← K(J)
SOLV FOR
ISMALL,IBIG
11
SETL1, L2, L3,L4
A

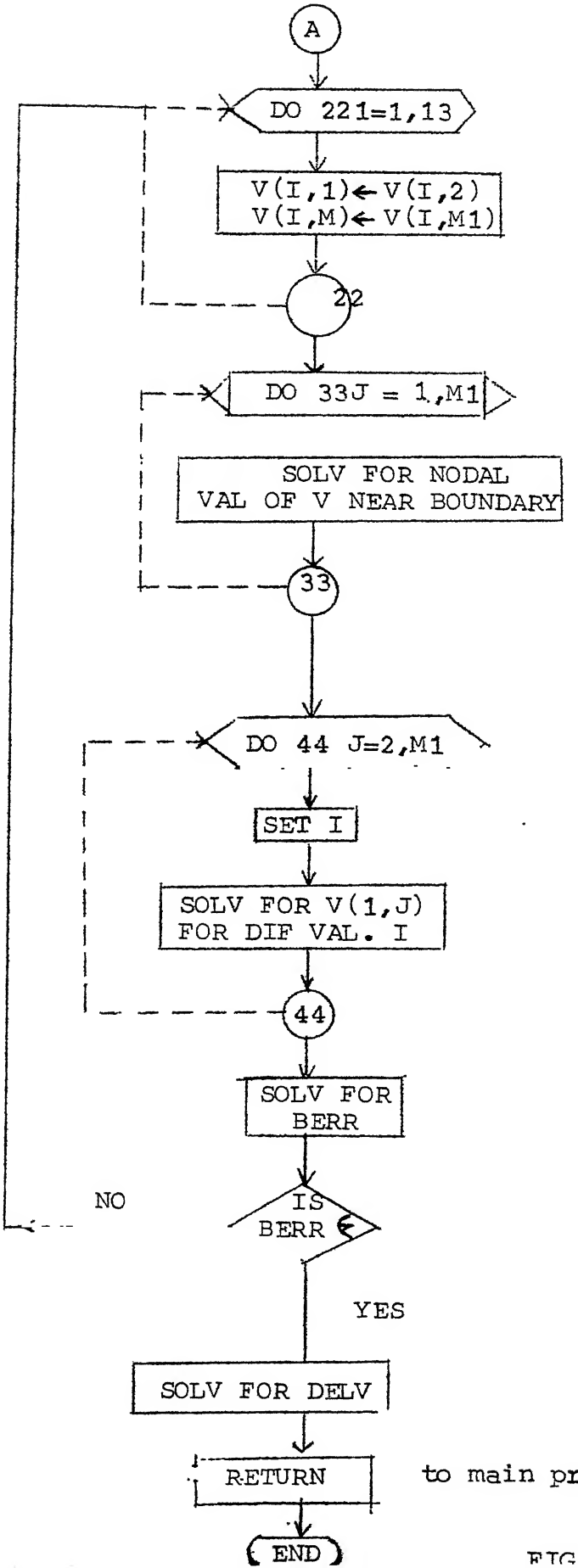
A
DO 221=1,13
V(I,1)← V(I,2)
V(I,M)← V(I,M1)
22
DO 33J = 1,M1
SOLV FOR NODAL
VAL OF V NEAR BOUNDARY
33
DO 44 J=2,M1
SET I
SOLV FOR V(1,J)
FOR DIF VAL. I
44
SOLV FOR
BERR
NO
IS
BERR
YES
SOLV FOR DELV
RETURN
to main programme
END

FIG. 2.24

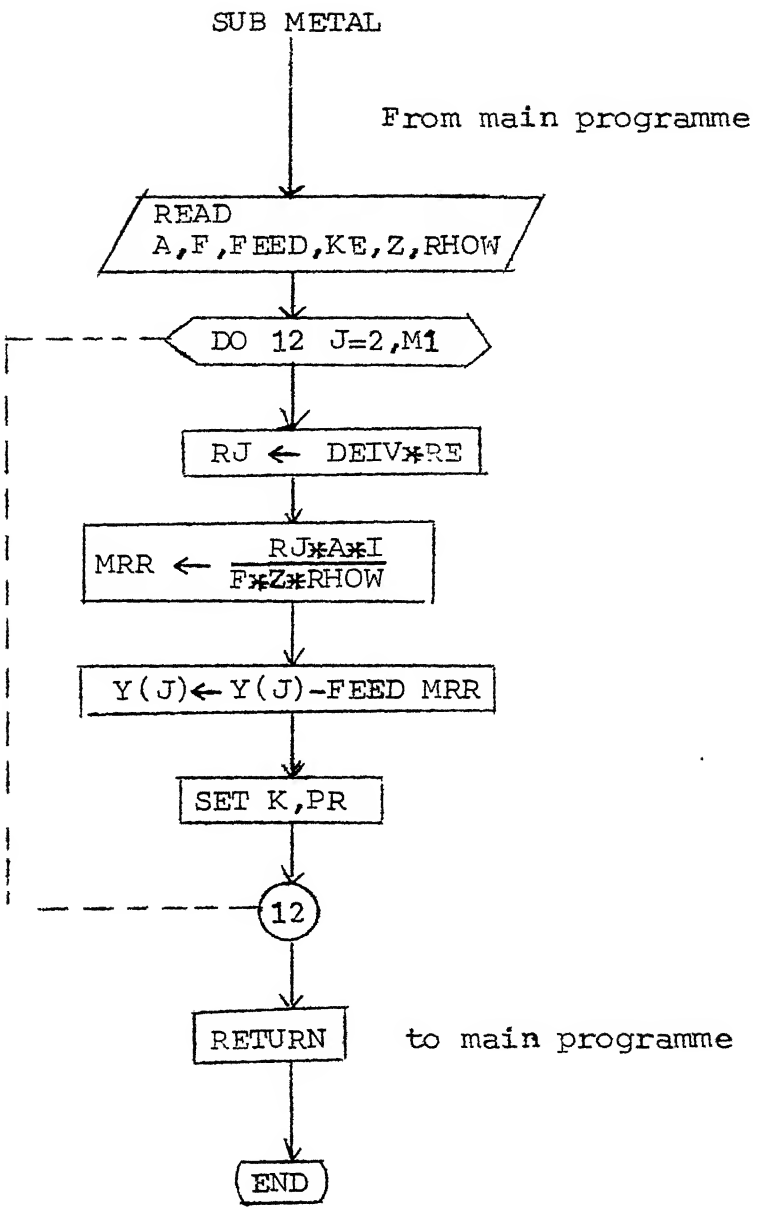
SUB METAL
From main programme
READ
A,F,FEED,KE,Z,RHOW
DO 12 J=2,M1
RJ ← DEIV*RE
MRR ← RJ*A*I / F*Z*RHOW
Y(J)← Y(J)-FEED MRR
SET K,PR
12
RETURN
to main programme
END

FIG. 2.25

In the present analysis the annular composite tool (cathode) was kept at zero volts. And the circular workpiece (anode) was given a voltage of 10 volts. The composite tool was separated from the anode by an initial gap of 0.5 mm.

Then by varying the machining times applied to the sections 1, 2 and 3 (Fig. 2.11), different work-geometries have been obtained.

(i) In this case the voltage applied to all the sections was 10 V. But the duty cycles for the segments 1,2 and 3 were 9 sec., 6 sec. and 3 sec., respectively. Thus the total duty cycle was fixed as 18 sec. The initial gap was divided into a mesh of size 0.1 x 0.1 mm^2, Fig. 2.22. The above data was fed to the programme to determine the amount of dissolution under each segment. The new anode boundary obtained formed a new boundary of the region between the electrodes.

As the feed was zero in this case, the cathode boundary was not displaced. The profile of the anode surface obtained after each full cycle has been plotted (Fig. 2.26). The analysis was conducted for a total of 8 cycles. As can be observed from Fig. 2.26, the amount of machining varies in accordance with the duty cycle for each segment.

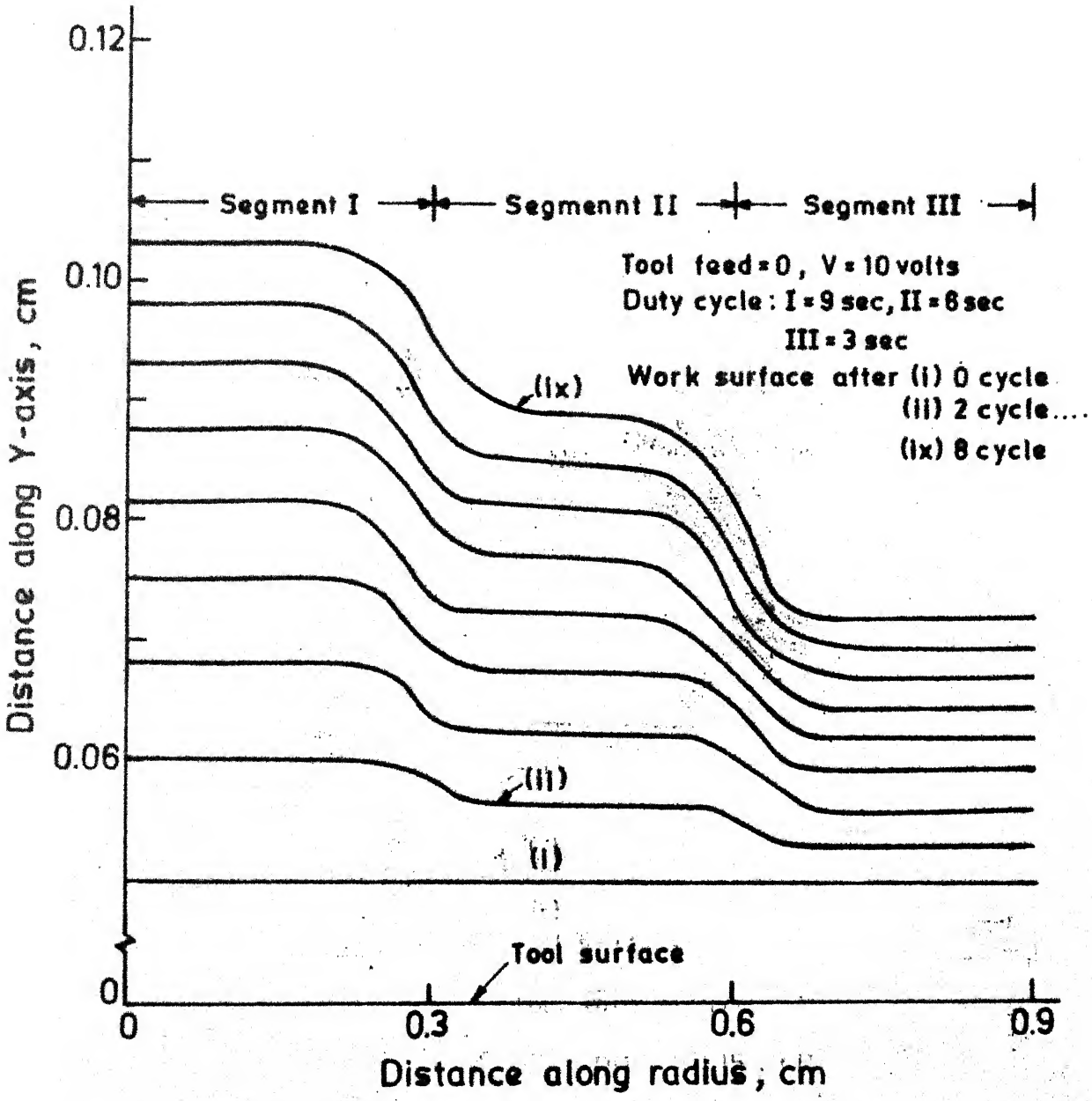

Fig. 2.26 Variation of Worksurface with Dutycycle (Theoretical)

(ii) In the second case, effectively there were two segments. The voltage was applied to the segment 1 for 3 s while the voltage was applied to the segment 2 and 3 for 6 s. The same process of computation was used to obtain the configuration of the workpiece. The results for 8 cycles are as shown in Fig. 2.27.

(iii) In this case the effect of the feed was also incorporated. A feed of 0.018 mm/cycle was given to the cathode. The duty cycle for each segment was different. As shown in Fig. 2.28 ,it was 3 s for the segment 1, 6 s for the segment 2 and 9 s for the segment 3.

The computation was done upto the eighth cycle. It can be observed from Fig. 2.28 that the worksurface is approaching a steady shape.

2.3 CASE:2 SQUARE COMPOSITE TOOL:

In the present work an additional composite tool has been suggested to generate the cavities or the work-geometries which are not axisymmetric. The composite tool under consideration consists of square faced pieces of copper. Each piece is separated from the other by a thin coating of insulating material. The tool contains an eight by eight matrix of such elements (Fig. 2.12). Each element is separately connected to the negative side of the power supply. By designing a proper control

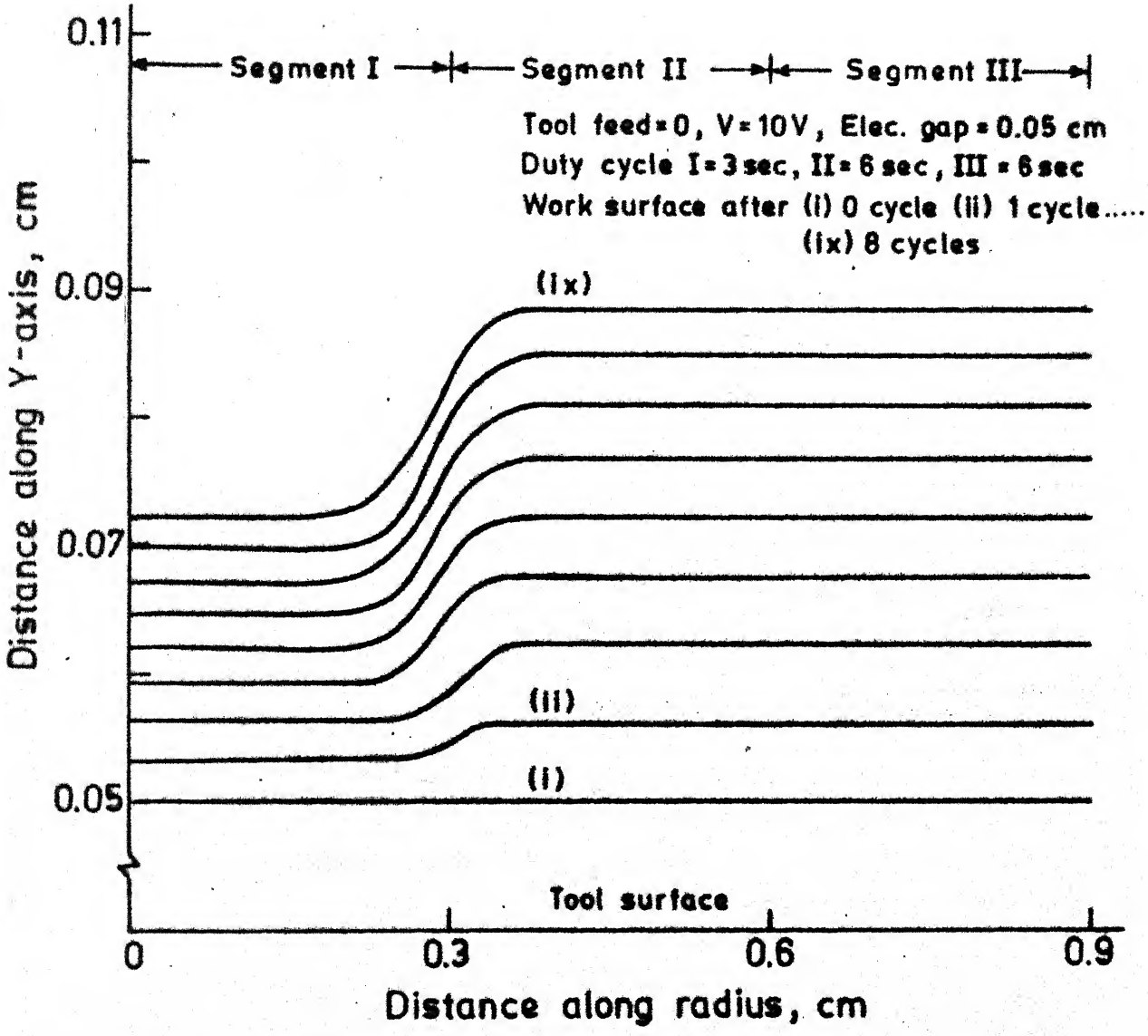

Fig. 2.27 Variation of Worksurface with duty cycle (theoretical)

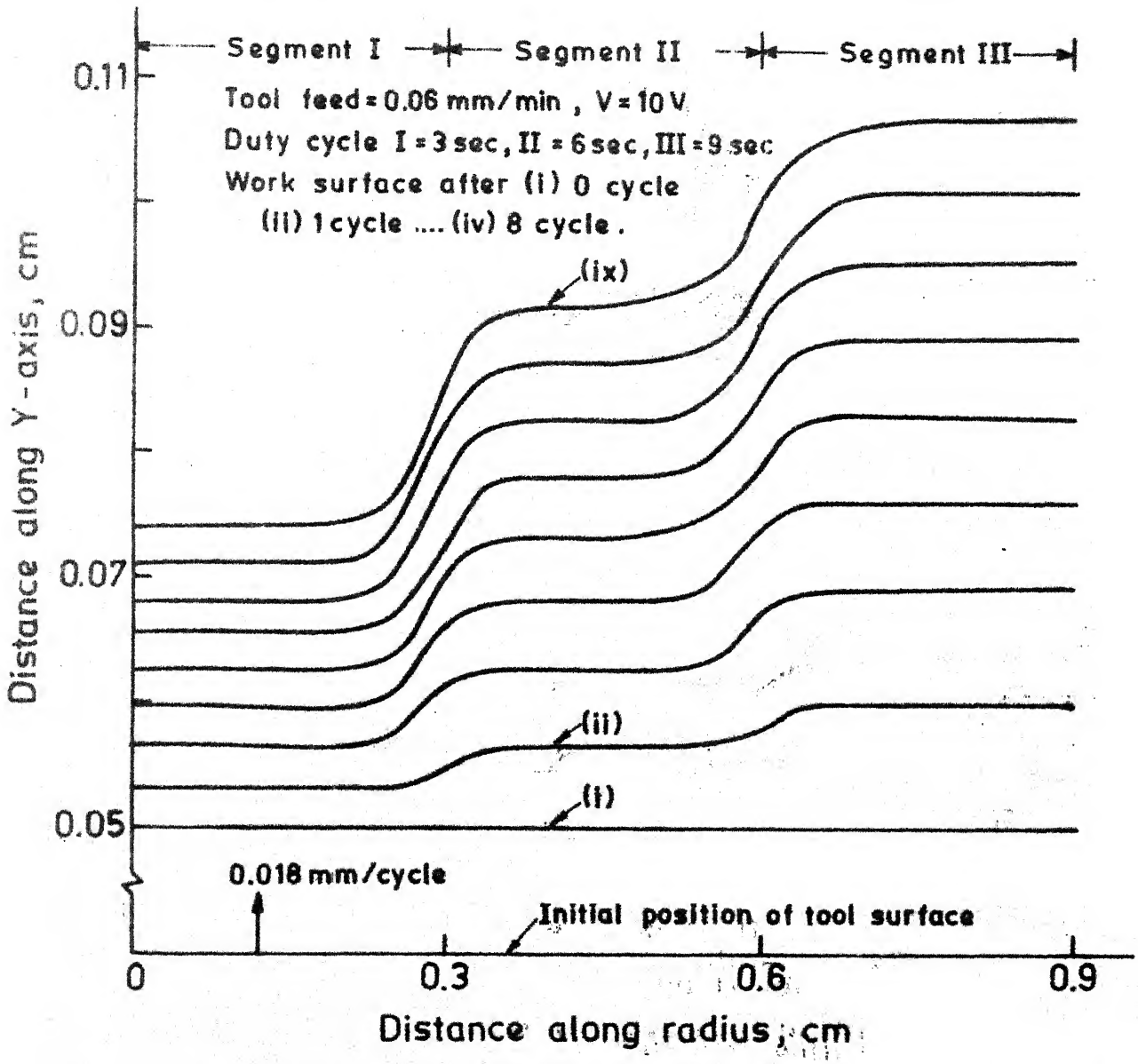

Fig. 2.28 Variation of Worksurface with Dutycycle (Theoretica

circuit, each element of the cathode can be connected to the circuit for different intervals of time. A microprocessor will be needed to control the duty cycle of each element.

The use of different duty cycles for each element will result in varying amount of the metal removal under each tool piece. Thus, this composite tool can be used to produce different shapes.

Here also, it is essential to obtain the potential distribution across the electrode gap to predict the final configuration of the worksurface. The potential distribution can be found by solving the Laplace's equation for specified boundary conditions. The Laplace's equation in the three dimensional form is as follows:

$$\frac{\partial^2 \phi}{\partial x^2} + \frac{\partial^2 \phi}{\partial y^2} + \frac{\partial^2 \phi}{\partial z^2} = 0 \qquad 2.31$$

As in the case of the annular tool, the numerical solution to this equation requires specification of the coordinates of both the cathode and the anode surfaces. In this case, the coordinates have been defined by an equispaced cubical mesh (Fig. 2.31a). Each grid point is specified by a set of coordinates i, j and k (Fig. 2.31b).

The simplified form of the Laplace's equation using the finite difference method can be written as;

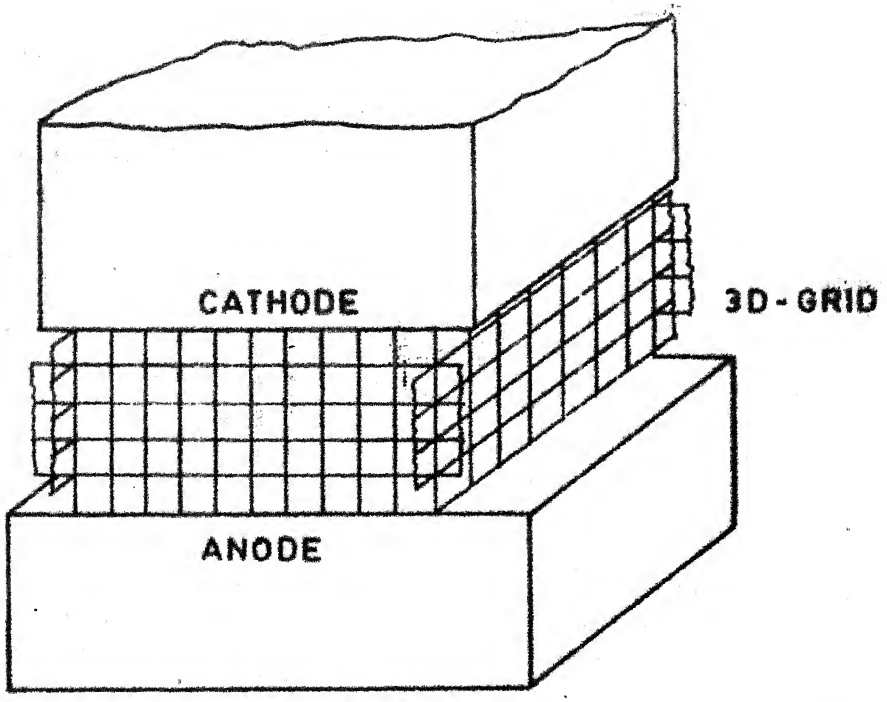

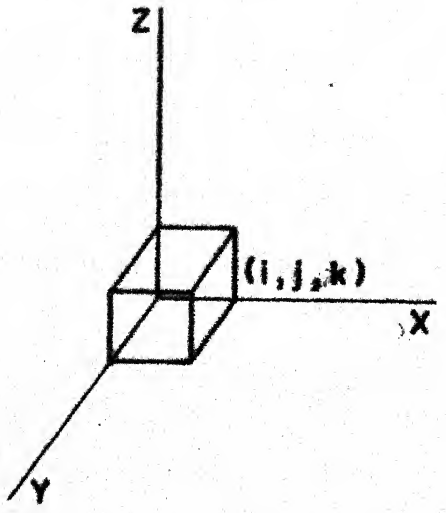

Fig. 2.31 Grid pattern in three dimensional case.

$$\phi(i+1, j, k) + \phi(i-1, j, k) + \phi(i, j+1, k) + \phi(i, j-1, k) + \phi(i, j, k+1) + \phi(i, j, k-1) - 6\phi(i, j, k) = 0 \qquad 2.32$$

where $\phi(i,j)$ is the potential at a grid point.

The details of the derivation of equation are given in Appendix B. From equation (2.32) it is clear that if the potential at the 6 neighbouring points are known then the potential at a point can be estimated.

The boundary conditions in this case are specified as follows:

(1) the potential at the grid points on the cathode is taken as 0 Volts,

(2) the potential at the grid point on the anode are fixed at a specified value V (which is 10 V. in the present case),

(3) $\frac{dv}{dx} = 0$ and $\frac{dv}{dy} = 0$ at grid points on the surfaces enclosing the mesh from the four sides. This condition is incorporated by applying mirror symmetry,

(4) $\frac{dv}{dz} = 0$, in the segment which is not connected in that particular time interval.

An initial value of the potential is assumed for all the grid points except the grid points on the

anode and the cathode. The above boundary conditions and the initial values when substituted in the following equation

$$[\phi(i+1, j, k) + \phi(i-1, j, k) + \phi(i, j+1, k) + \phi(i, j-1, k) + \phi(i, j, k+1) + \phi(i, j, k+1) + \phi(i, j, k-1)] - 6\phi(i, j) = R$$

Yields a value of R which indicates the deviation by which the assumed potential distribution differs from the correct potential distribution. The maximum value of R over the field is minimized to get the final solution.

From this potential distribution, grad (ϕ) can be found out. Then using equation (2.21) the amount of material dissolved can be computed.

Due to the dissolution of metal from the anode surface, the boundary gets displaced. The new anode surface may no longer contain the grid points. The linear interpolation is used to evaluate the potential distribution on the grid points near the anode surface.

Repeating the same process, depth of cut for a finite time is determined. The computation is repeated till the change in the shape of the anode surface becomes negligible.

The above steps have been incorporated in a program. The flow charts illustrating the programme are

shown in Figs. 2.32, 2.33, 2.34, and 2.35.

This analysis was restricted to one quadrant of the composite tool. This was done for the ease of computation. The surfaces which have been generated are symmetric in shape. This surface pattern obtained can easily be extended to all the quadrants. The size of each element was fixed as 1 x 1 mm^2.

The following two cases were taken up:

(i) Four segments were identified on the tool as shown in Fig. 2.36. The duty cycles for the segments 1, 2, 3 and 4 were set as 3 s, 6 s, 9 s and 12 s, respectively. The full cycle time was 12 s. The electrode gap was initially set as 0.5 mm. The space between the tool and the workpiece was divided into a mesh of 0.1 x 0.1 x 0.1 mm^3 size.

The above data, when fed to the program gave the electrode gap after each cycle. A specified feed of 0.03/cycle was also incorporated at the end of each cycle. The isometric view drawn from the results, obtained after the 8th cycle, is shown in Fig. 2.37.

(ii) As shown in Fig. (2.38), the tool was divided into eight segments. The duty cycle for each segment was as shown in the figure. The total cycle time was 16 s.

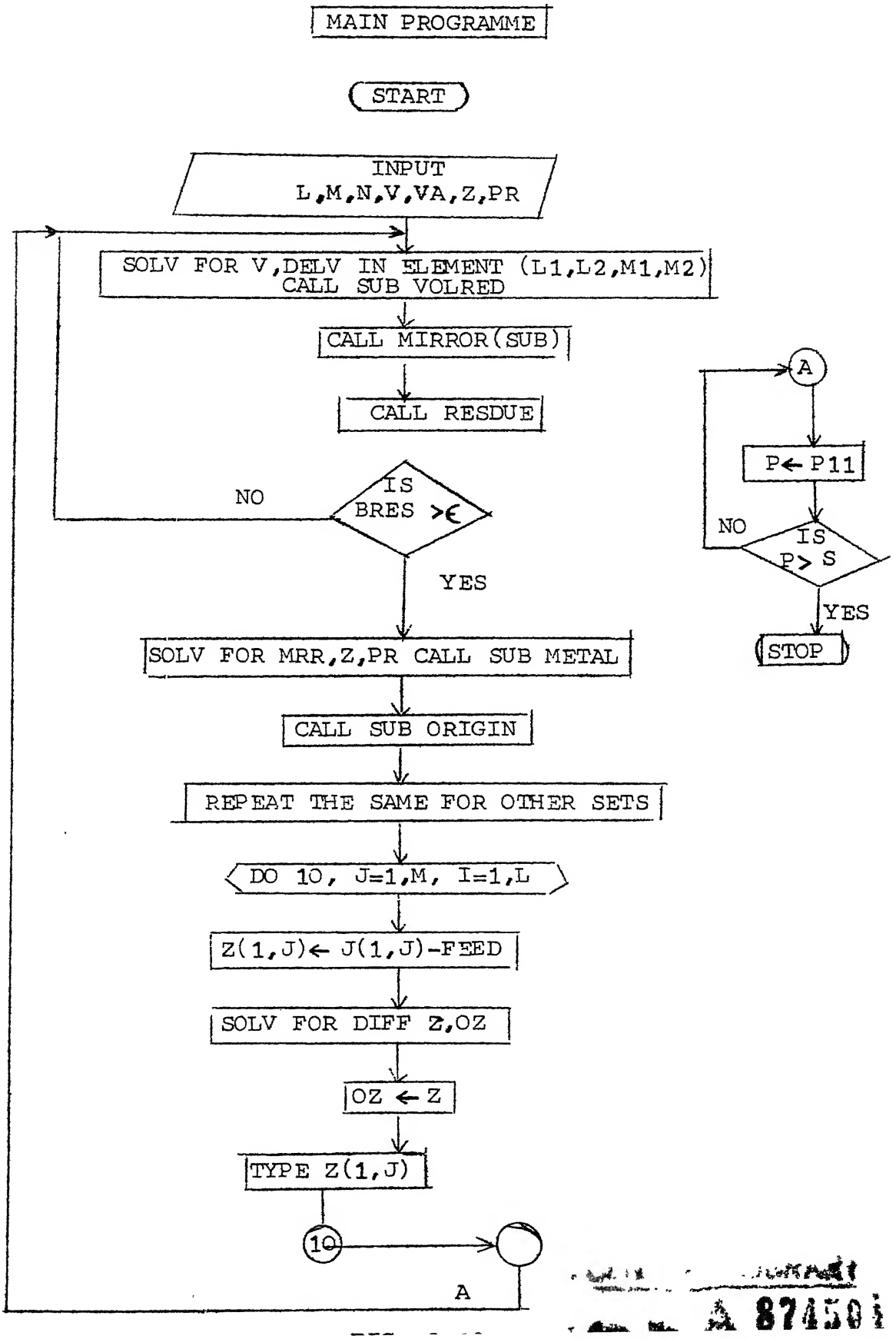
MAIN PROGRAMME
START
INPUT
L,M,N,V,VA,Z,PR
SOLV FOR V,DELV IN ELEMENT (L1,L2,M1,M2)
CALL SUB VOLRED
CALL MIRROR(SUB)
CALL RESDUE
IS
BRES >€
NO
YES
SOLV FOR MRR,Z,PR CALL SUB METAL
CALL SUB ORIGIN
REPEAT THE SAME FOR OTHER SETS
DO 10, J=1,M, I=1,L
Z(1,J)← J(1,J)-FEED
SOLV FOR DIFF Z,OZ
OZ ← Z
TYPE Z(1,J)
10
A
A
P← P11
NO
IS
P> S
YES
STOP

A 87450i

SUB VOLRED

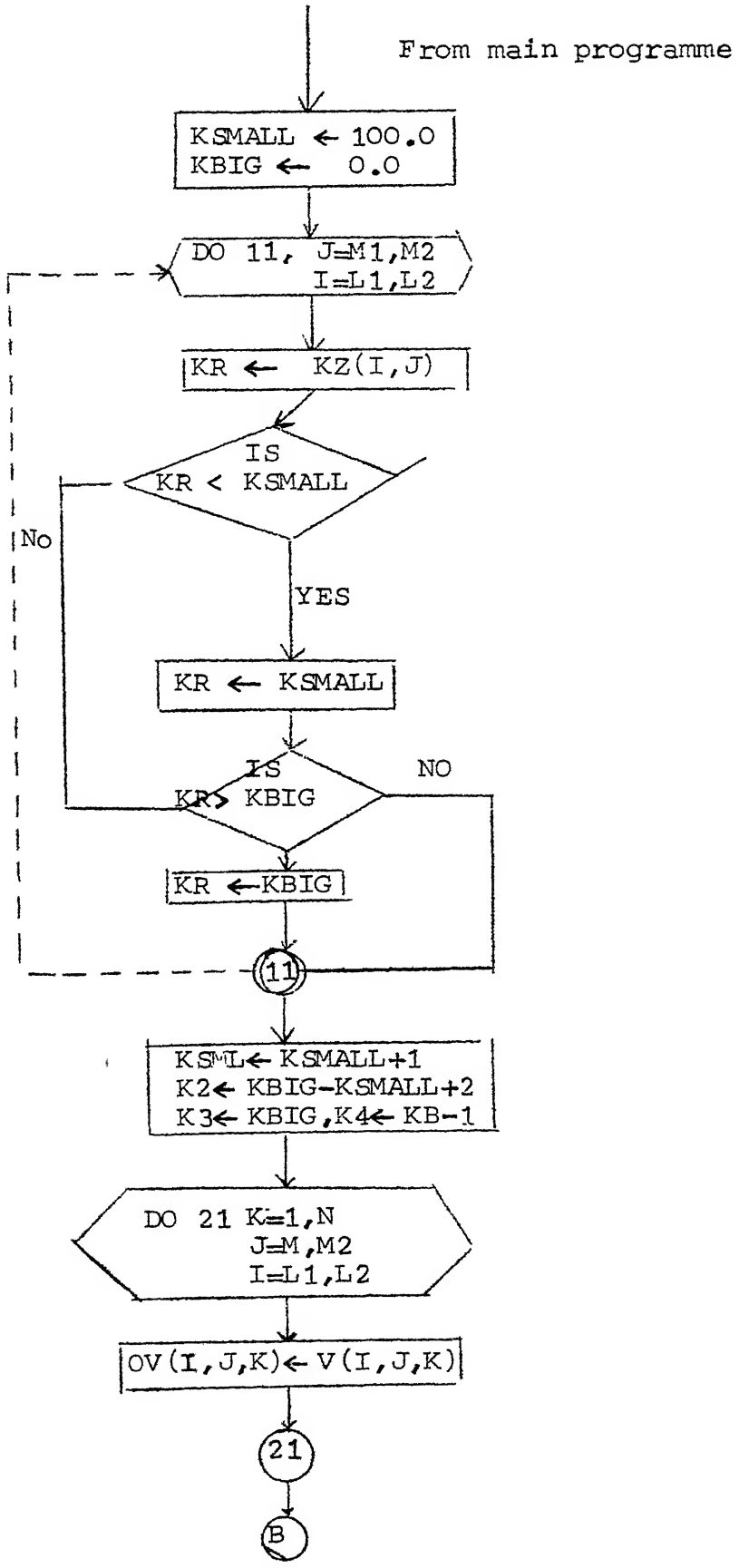
From main programme
KSMALL ← 100.0
KBIG ← 0.0
DO 11, J=M1,M2
I=L1,L2
KR ← KZ(I,J)
IS
KR < KSMALL
No
YES
KR ← KSMALL
IS
KR > KBIG
NO
KR ←KBIG
11
KSML← KSMALL+1
K2← KBIG-KSMALL+2
K3← KBIG, K4← KB-1
DO 21 K=1,N
J=M,M2
I=L1,L2
OV(I,J,K)← V(I,J,K)
21
B

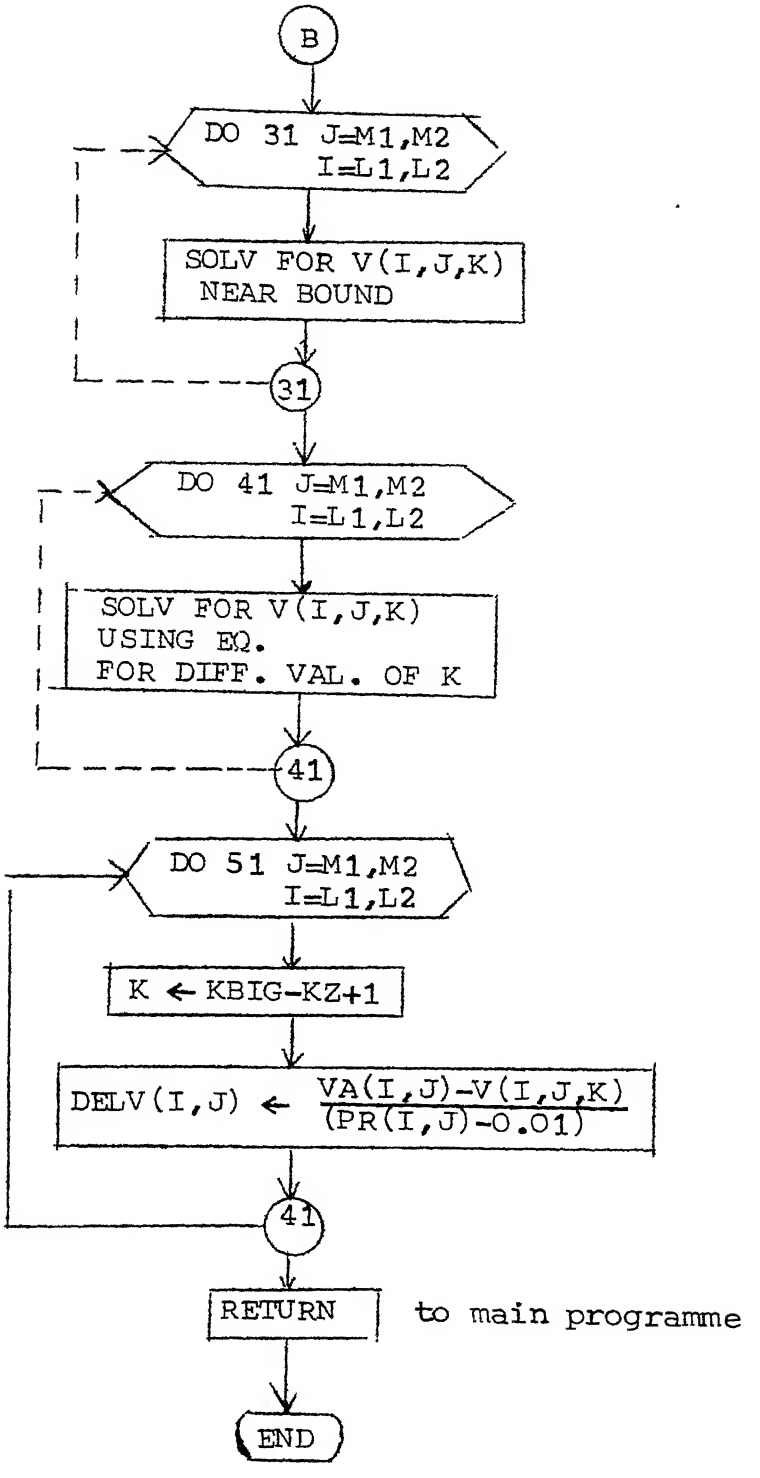
B
DO 31 J=M1,M2
I=L1,L2
SOLV FOR V(I,J,K)
NEAR BOUND
31
DO 41 J=M1,M2
I=L1,L2
SOLV FOR V(I,J,K)
USING EQ.
FOR DIFF. VAL. OF K
41
DO 51 J=M1,M2
I=L1,L2
K ← KBIG-KZ+1
DELV(I,J) ← VA(I,J)-V(I,J,K) / (PR(I,J)-0.01)
41
RETURN
to main programme
END

FIG. 2.33

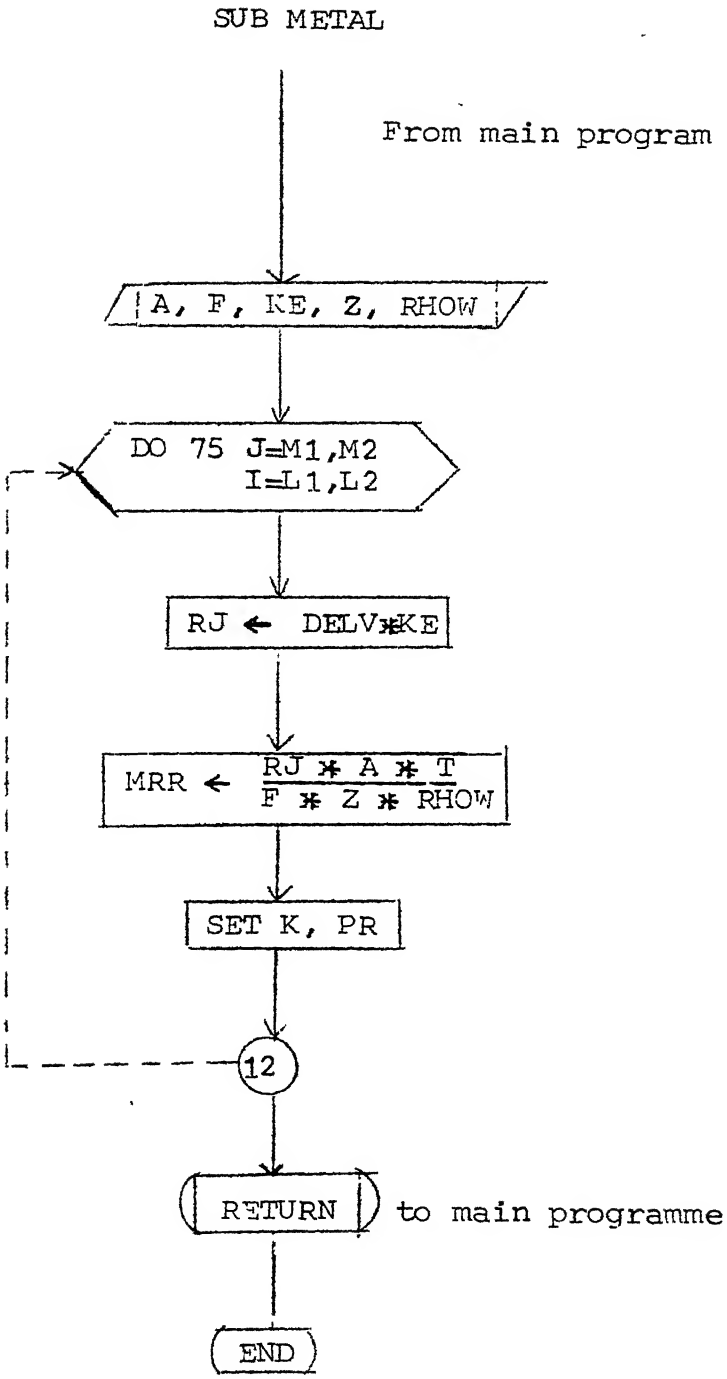
SUB METAL
From main program
A, F, KE, Z, RHOW
DO 75 J=M1,M2
I=L1,L2
RJ ← DELV*KE
MRR ← RJ * A * T / F * Z * RHOW
SET K, PR
12
RETURN
to main programme
END

FIG. 2.34

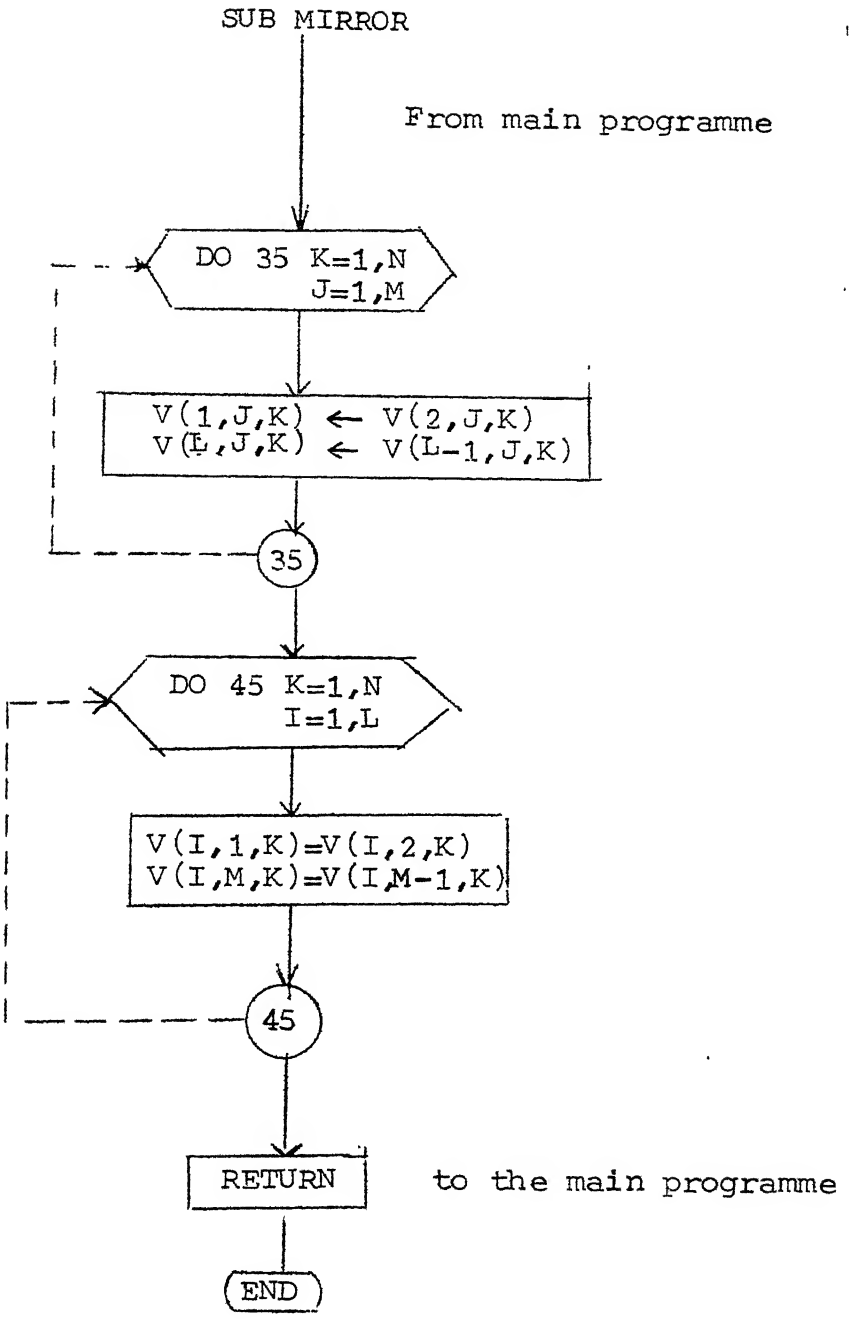
SUB MIRROR
From main programme
DO 35 K=1,N
J=1,M
V(1,J,K) ← V(2,J,K)
V(L,J,K) ← V(L-1,J,K)
35
DO 45 K=1,N
I=1,L
V(I,1,K)=V(I,2,K)
V(I,M,K)=V(I,M-1,K)
45
RETURN
to the main programme
END

FIG. 2.35a

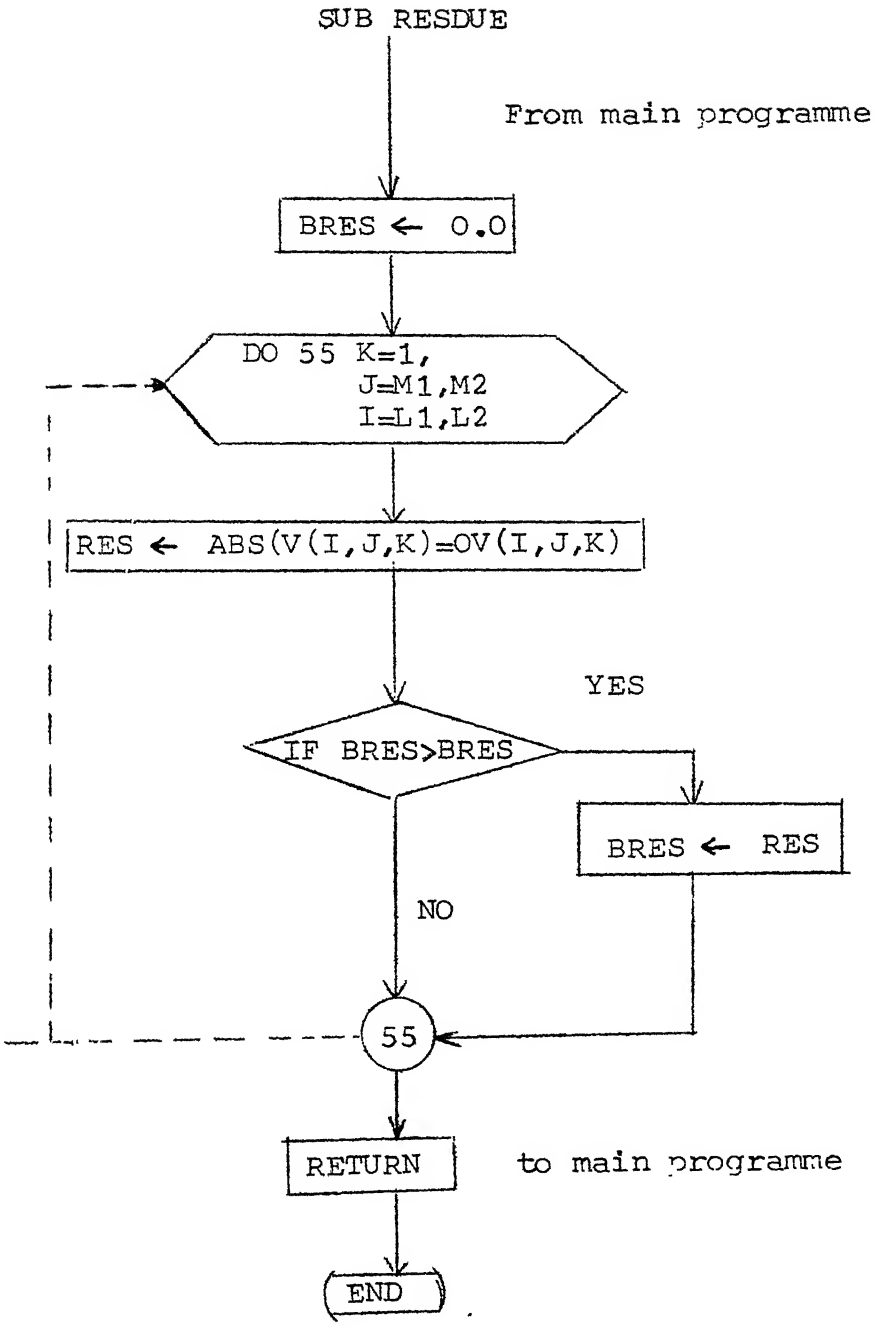
SUB RESDUE
From main programme
BRES ← 0.0
DO 55 K=1,
J=M1,M2
I=L1,L2
RES ← ABS(V(I,J,K)=OV(I,J,K)
YES
IF BRES>BRES
BRES ← RES
NO
55
RETURN
to main programme
END

FIG. 2.35b

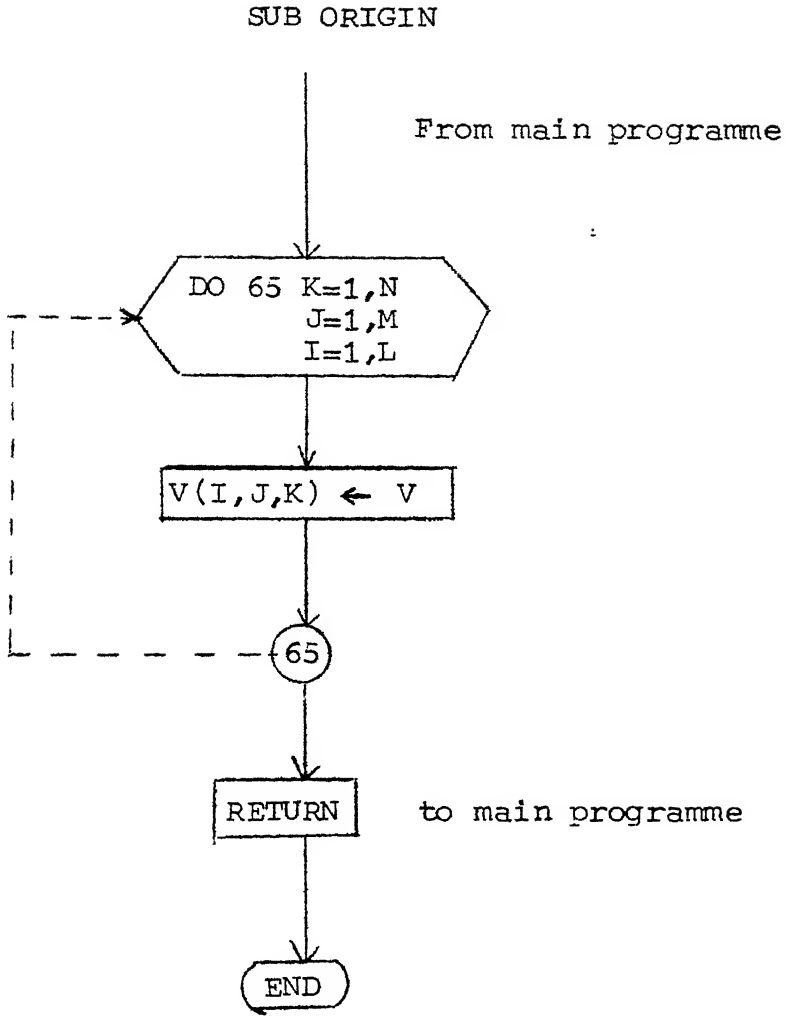
SUB ORIGIN
From main programme
DO 65 K=1,N
J=1,M
I=1,L
V(I,J,K) ← V
65
RETURN
to main programme
END

FIG.2.35c

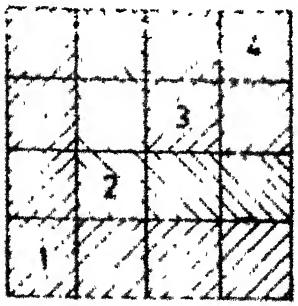

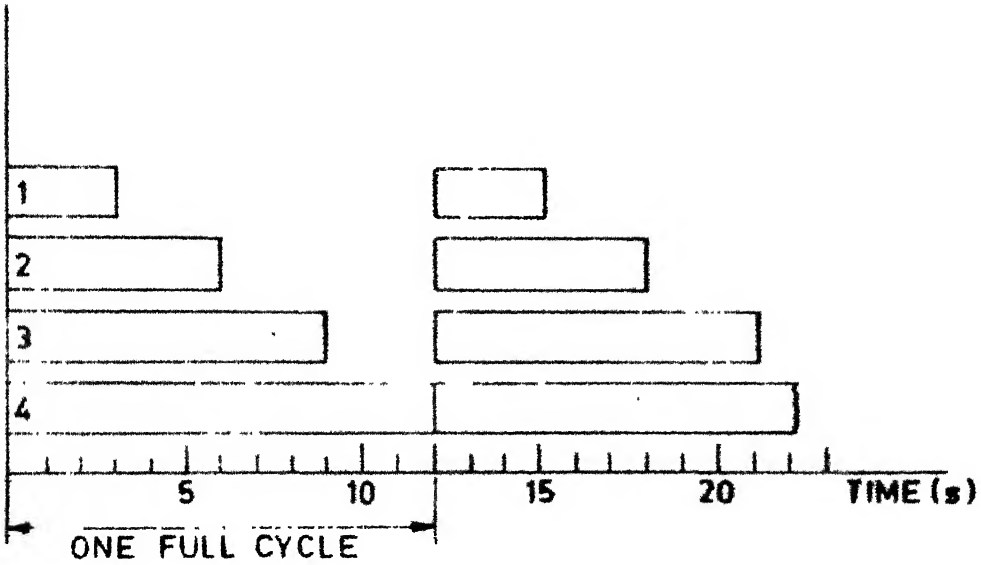

Fig. 2.36 (a) Tool Configuration (1)
(b) Duty cycle for Different sections.

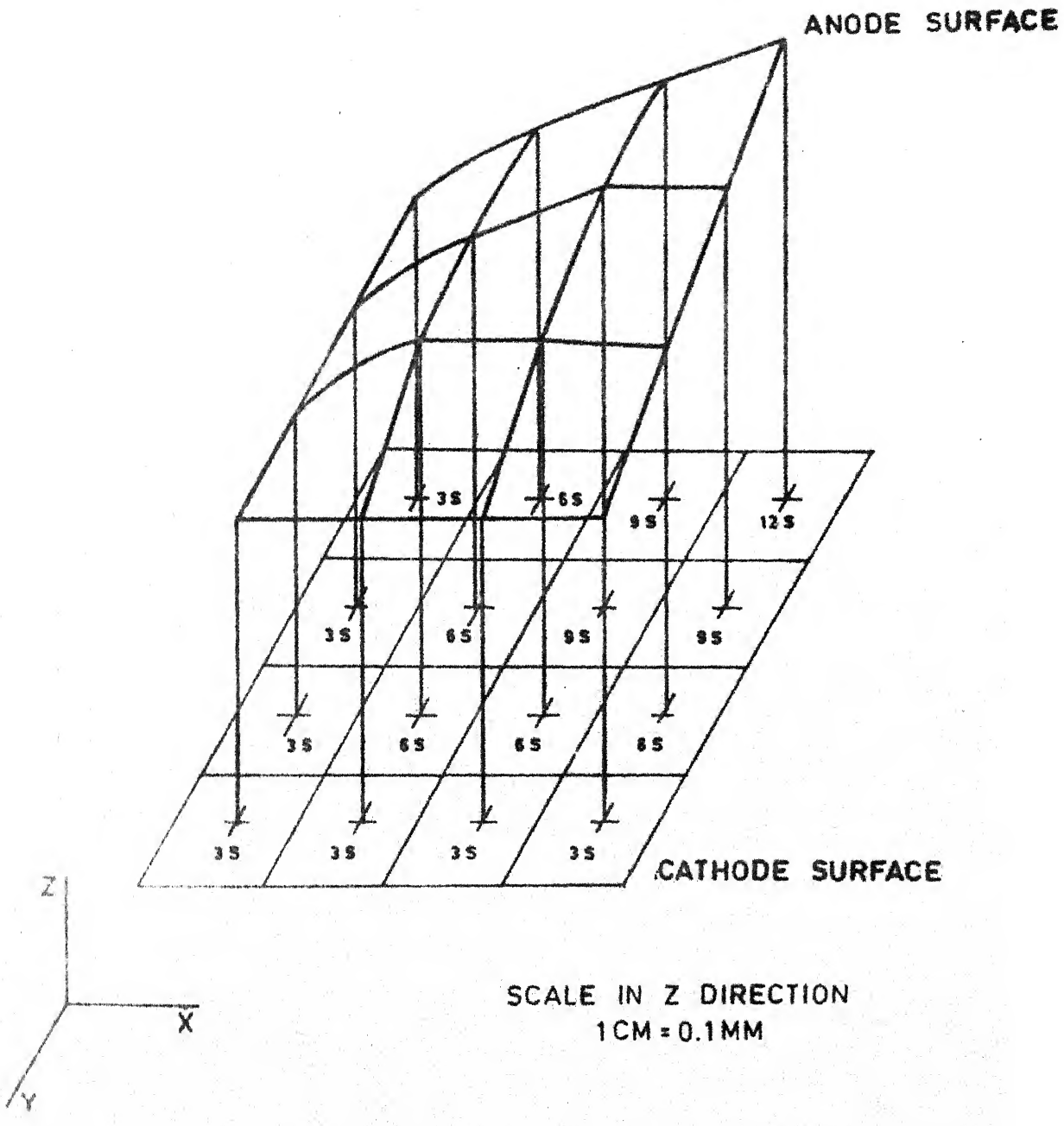

Fig. 2.37 Isometric View of Worksurface (1)

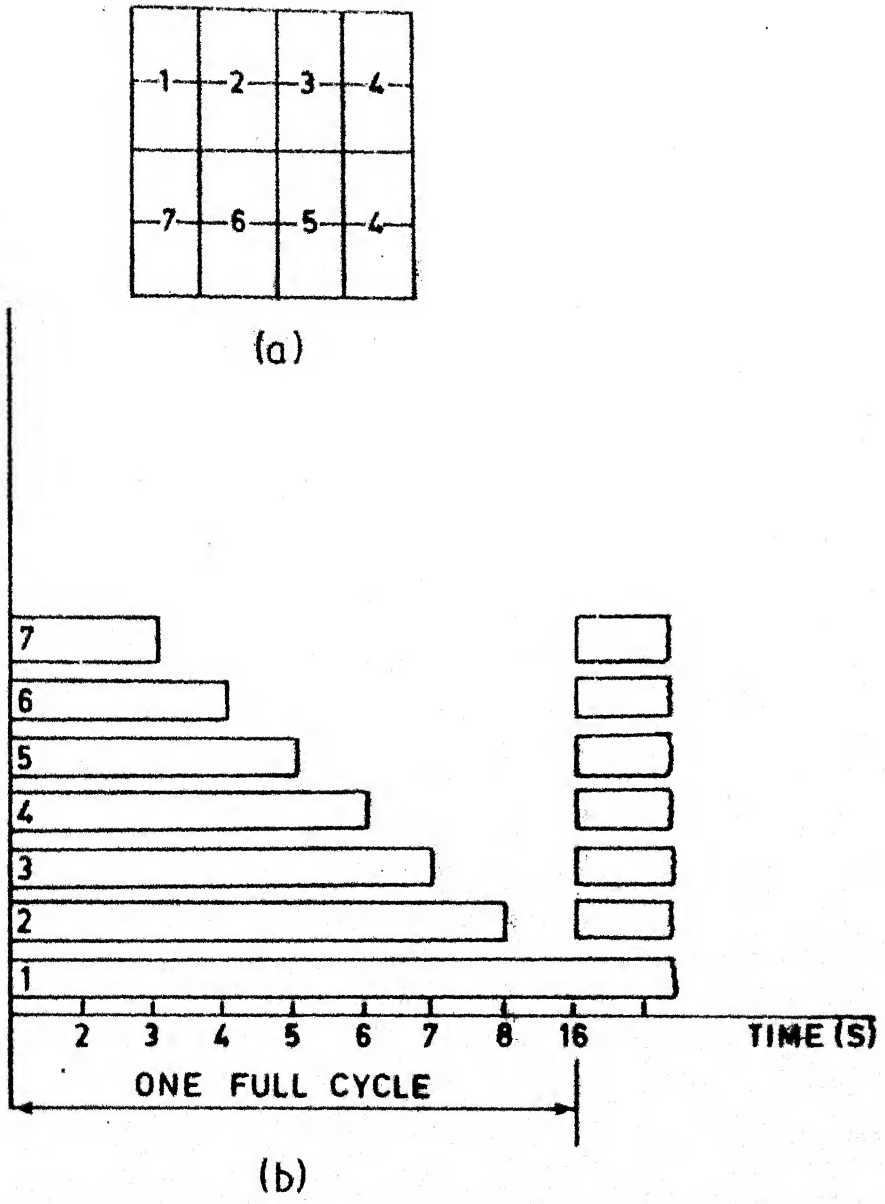

Fig 2.38 (a) Tool Configuration (2)
(b) Duty Cycle for Different sections.

The tool was moved by a distance of 0.06 mm. after the end of each cycle.

The mesh size used was same as that in the first case. Electrode gap after each cycle of machining was computed. The results obtained at the end of the eighth cycles have been used to draw the isometric view shown in Fig. 2.39.

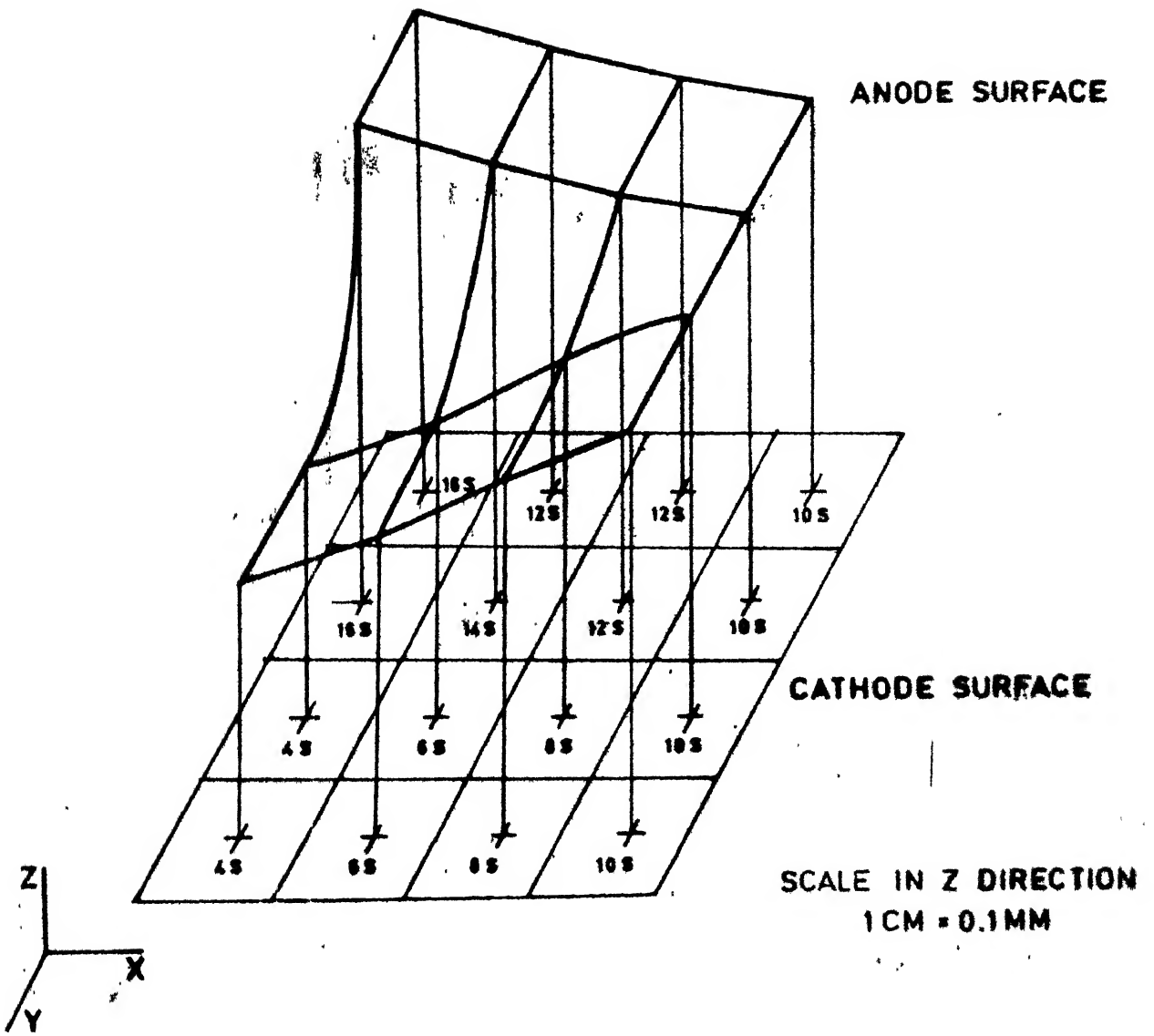

Fig. 2.39 Isometric View of Worksurface (2)

CHAPTER-3

EXPERIMENTAL DETAILS

3.1 INTRODUCTION:

A theoretical analysis has been described in the previous chapter. Here, the basic features of the experimental set-up havebeen discussed.

The schematic arrangement of the electrochemical machine is shown in Fig. (3.11). The tool which is fixed to the tool holder is connected to the negative terminal of the power source. And the workpiece which is mounted on the fixture is connected to the positive D.C. power supply and the fixture is insulated from the base. The electrolyte is passed through the hole, provided in the tool. The electrolyte which is splashed out from the gap between the electrodes is collected in the sink and recirculated. Tool is fed by means of a linear feeding device. A quick withdrawal system is provided. In this case the feed was controlled by a stepper motor through a EC-85 microprocessor.

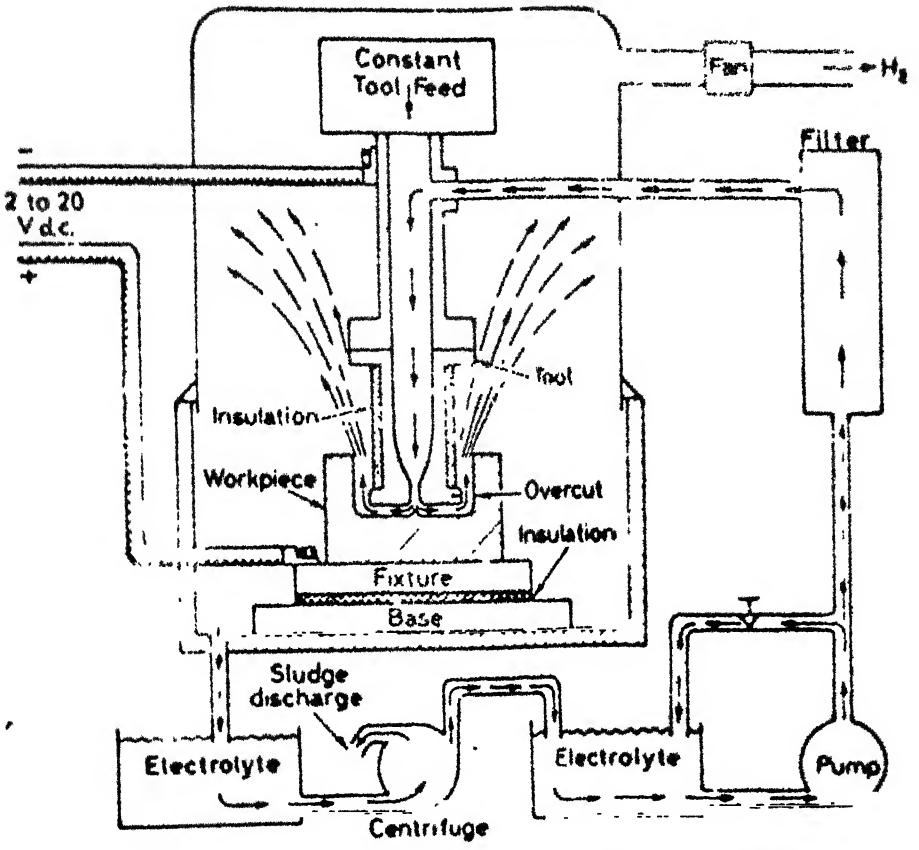

Fig. 3.1: *Schematic diagram of electrochemical machine*

3.2 COMPOSITE TOOL DESIGN:

In the present work the experiments have been restricted only to the axisymmetric case. And for this a cylindrical tool with annular sections has been designed. This is a three core tool as shown in Fig. (3.21). The tool has been designed with the aim to apply constant voltage to the different sections for different intervals of time.

The tool consists of three concentric cylinders of same thickness (2.5 mm) but of different lengths, inserted one inside the other. All the three layers were separated with an insulating material (Bakelite). A terminal was attached to each of the copper layers to supply the necessary voltage and current at the time of machining through a relay.

3.3 SWITCHING CIRCUIT:

In the present experiments, it is important to control the elements of the electrodes for individual timings. For synchronising the ON/OFF time of the three elements of the electrode, a switching circuit was designed using a monostable multivibrator. The circuit (Fig. 3.31) consists of NAND, NOR Gates, monostable multivibrator (retriggerable), drivers and relays. A monostable multivibrator is a flip-flop device but has one

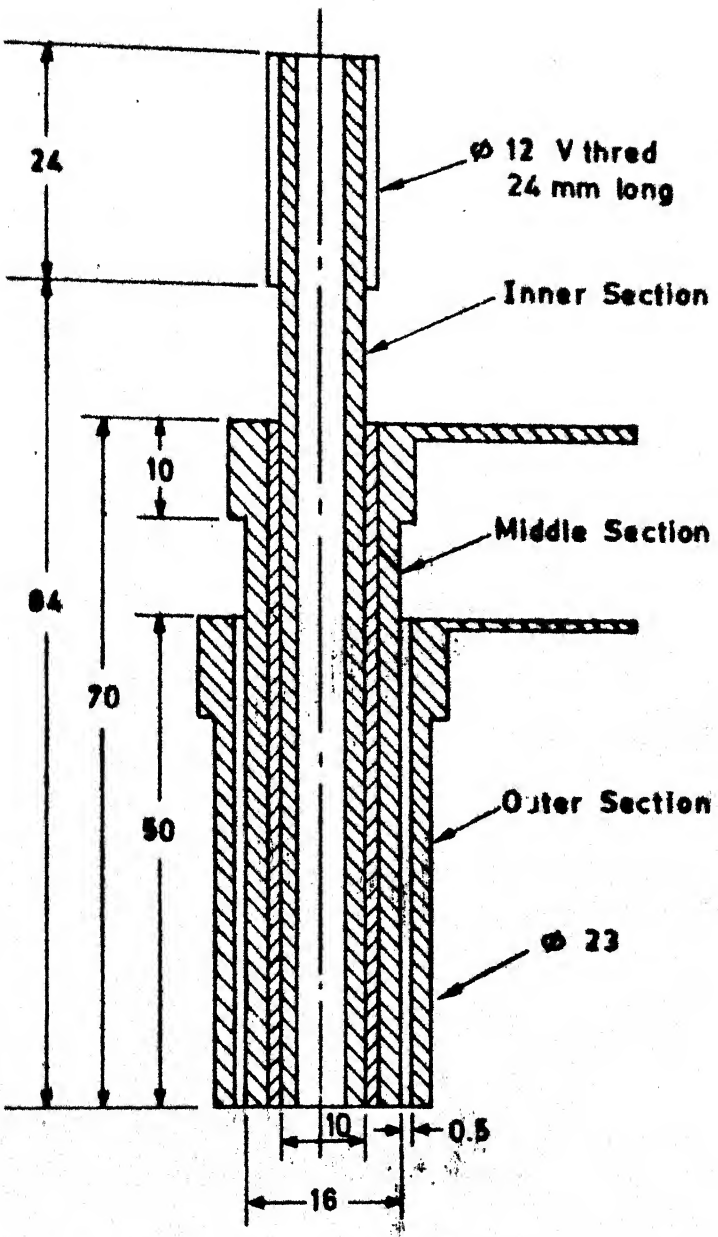

ALL DIMENSIONS ARE IN mm
SCALE 2:1

Fig. 3.21 Composite Tool

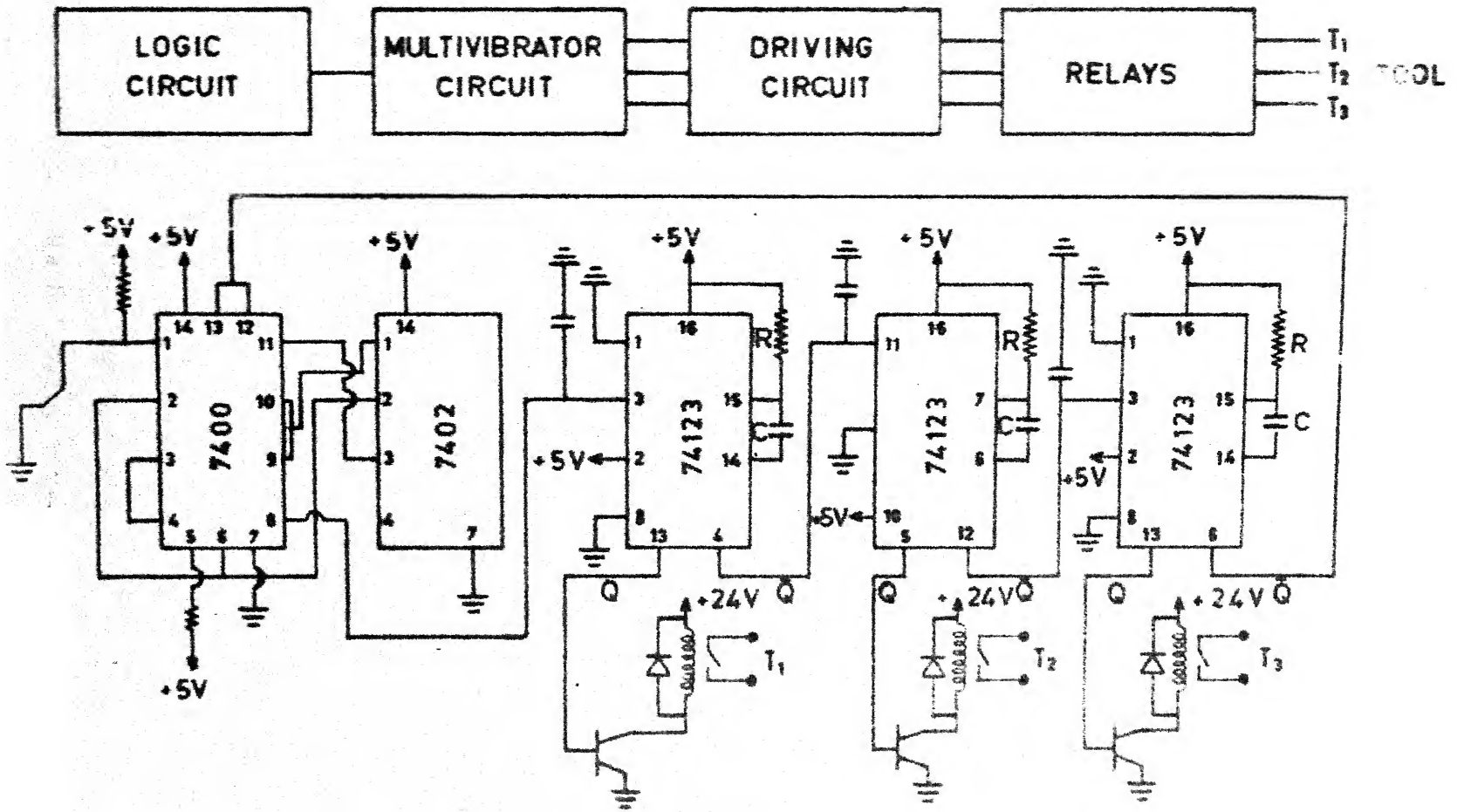

Fig. 3.31 Schematic Diagram of Timing Circuit.

stable state and one memory state. That is, when it is triggered, the output (Q) set to logic 1 and remains set for a predetermined length of time. When this period of time lapses, the output automatically returns to logic '0', and the device has then returned to its stable state. An external resistor and capacitor (R and C) which serves as timing components precisely determine the delay period. The complementary output ($\bar{Q}$) is used to trigger the second multivibrator (with another set of timing components) and so on. The output Q of predetermined time is fed to the driver circuit which inturn operates the relay switch. This process of triggering and retriggering goes on till the reset switch is pressed. For the present experiments the timing constants are chosen as 3 S, 6 S and 9 S in different combinations.

The Fig. 3.32 shows the various components of the experimental set up.

3.4 EXPERIMENTAL PROCEDURE:

To study the effect of the composite tool on anodic dissolution experiments were conducted on the ECM set up. Machining was carried on mild steel workpieces. A particular initial gap was adjusted to give the maximum dissolution. The following three experiments were conducted:

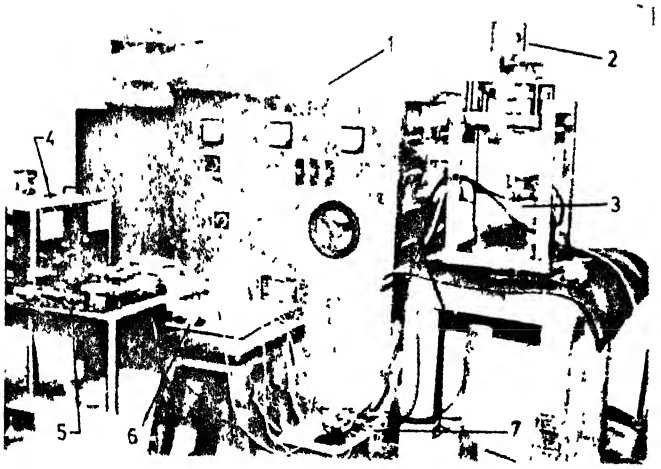

(1) Rectifier (20 V - 750 A DC)
(2) Stepper motor (3) Composite tool
(4) DC power supply (30 V - 10 A)
(5) EC-85 Microprocessor (7) Timing circuit
(8) Relays

Fig. 3.32. Experimental Set up

Expt.1. In this case the duty cycles were set in such a manner that the inner, middle and outer sections were kept on for 9 S, 6 S and 3 S respectively. The voltage was applied sequentially. The feed was kept zero. The initial gap was adjusted at 0.5 mm.

The depth of cut was measured after 25 minutes of machining. The profile was measured on M320 Carl Zeiss Profilometer. From Fig. 3.41 . it is clear that the depth of cut in different sections correspond to the duty cycles.

Expt.2. As shown in Fig. 3.41 on-time for the inner section was 3 S, where as the on-time for the other two sections was 6 S. The tool was not given any feed. The result obtained after 20 minutes of machining have been plotted (Fig. 3.41a).

Expt.3. The on-times for the inner, middle and outer sections were 3 S, 6 S and 9 S respectively. The tool was moved by a feed velocity of 0.6 mm/min after each cycle. The anode profile obtained after 15 minutes of machining is as shown in Fig. 3.41 .

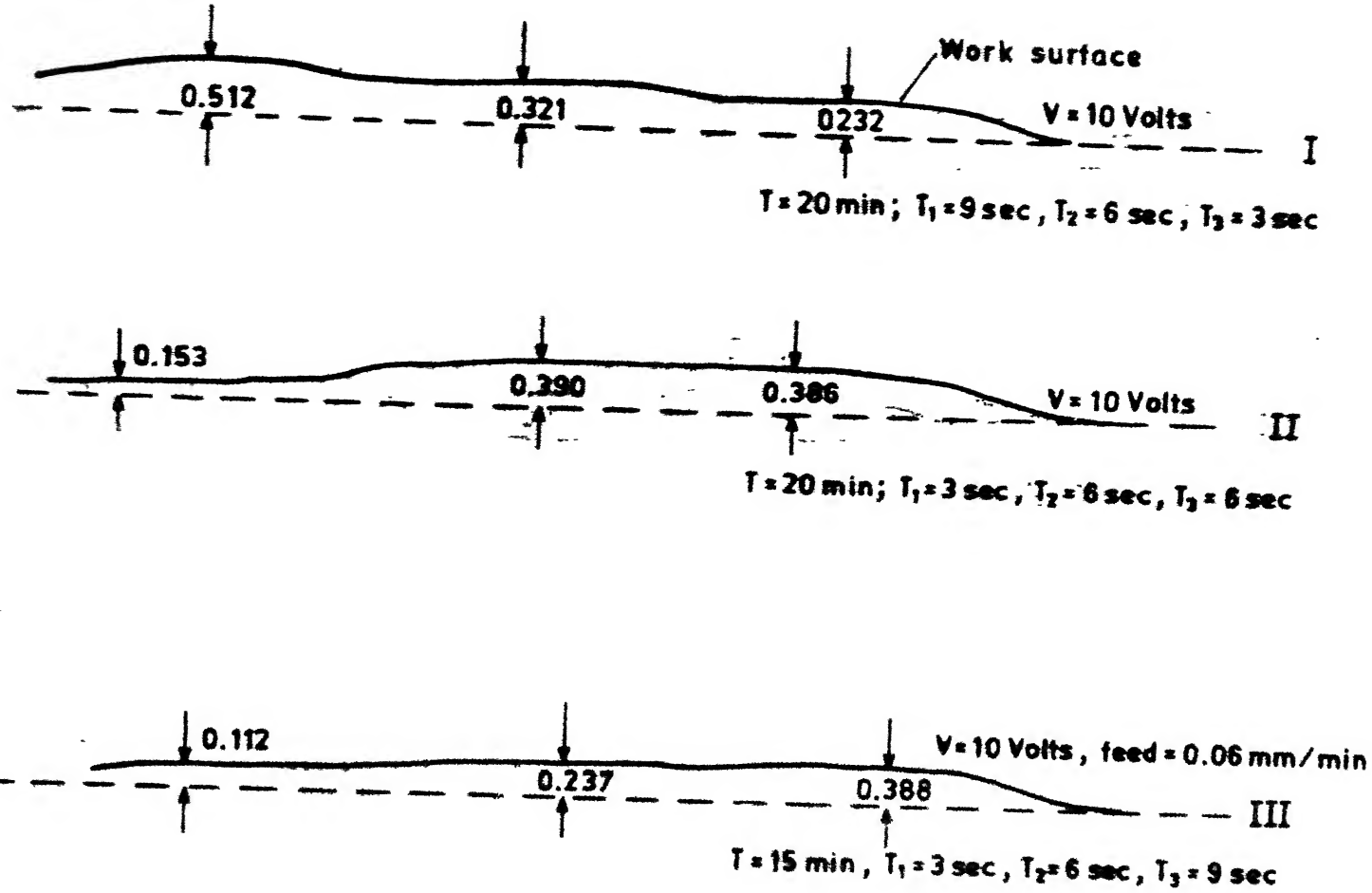

Fig. 3.41 Variation of worksurf- with Duty cycle (Experimental)

CHAPTER-4

RESULTS, DISCUSSIONS AND CONCLUDING REMARKS

The results of the theoretical analysis of the annular tool for three different working conditions are given in Figs.2.26, 2.27 and 2.28. In all these cases, the variation in the worksurface was achieved by suitably controlling the duty cycle of the individual tool segments.

Figs. 2.27 and 2.28 show the first two cases. In both the cases the tool was not provided with any feed motion. It is clear from the profiles obtained after each cycle that the amount of material removed depends on the duty cycle. The experimental results were obtained under the same conditions for which the theoretical analyses were conducted. Fig. 3.41a shows the experimentally generated worksurface. From the experimental results, it is clear that the amount of machining under each segment is proportional to the on-times. However, it was not possible to match the experimental and theoretical results very closely as the theoretical results were not computed for the total time used in the actual operation (in case of zero feed a stable work configuration cannot be obtained).

In the third case, a feed of 0.018 mm/cycle (0.6 mm/min) is also associated with the tool. It is seen again that the depth of cut varies as expected along the radius (Fig. 2.28). From Fig. 2.28, it is clear that the worksurface is gradually approaching a steady configuration. Fig. 3.41b shows the experimental results for similar conditions for which the theoretical analysis was done. It can be seen that the ratios of the step heights correspond to the respective on-time ratios (Fig. 3.41b).

The variations of the theoretically obtained worksurface are sharp where as the steps are smoother in the experimental case. This may be due to the fact that the insulation thickness in the composite tool was 0.5 mm, where as in the analytical model it was assumed to be zero.

The theoretical results obtained for the square composite tool are given in Figs. 2.37 and 2.39. In the first case, the duty cycle for each segment was as shown in Fig. 2.36. The isometric view, shown in Fig. 2.37, was drawn from the results obtained after the eighth cycle. It can be seen that the depth of cut under each element is in accordance with the duty cycle. The shape of the anode predicted for one quadrant of the tool indicates that when extended to the complete tool, a diamond shaped cavity will be obtained.

In the second case the isometric view (Fig. 2.39) shows two parallel slots. The depth of cut increases from one end to the other end of the slot. But the slope and the depth of the two slots are different. The above surface was achieved due to the different duty cycles used for the different segments.

In the three dimensional as well as the axisymmetric case, it is obvious that once the cavity is formed on the worksurface, the electrode gap no longer remains uniform. This will result in the separation and the cavitation during the electrolyte flow. Therefore, care should be taken to design the electrolyte flow to avoid turbulence, separation and vortices.

From the present work it can be noted that the time of machining is one definite parameter which affects the material removal rate. Thus by applying a constant voltage with a combination of different duty cycles in the elements of the composite ECM tool, various patterns could be obtained.

In case of the composite tool with large number of elements, accurate control of the profile of the worksurface can be achieved. A microprocessor should be used to control the potential duty cycles of the individual elements. Any desired shallow engraving can be obtained

by feeding a proper programme to the micro-processor. Apart from the direct use, this technique can be employed for making finer adjustments in the workgeometry machined by some other process.

In the present work, effects of many important parameters, such as the electrolyte flow, the overpotential, change in the electrolyte conductivity etc. have not been included. Still, the results show that it is practicable to use the proposed new concept.

REFERENCES

(1) Amitabha Ghosh, " Keynote Address", 10th AIMTDR Conference, Durgapur, Dec. 1932, p. 1.

(2) McGeough, J.A., Fitz-Gerald, J.M. and Marsh, L.M, J. Inst. Math. and Applics, 5, 1969, p. 409.

(3) Collet, D.E. Hewson-Browne, R. C, and Windle, D.W., J. Eng Math, 4, 1970, p. 29.

(4) Tipton, H and Tsuei, Y.G., Trans. ASME, Paper No. 76-WA/Prod. 1977, p. 1.

(5) Hewson-Browne, R.C., J. Engg. Math , 5, 1971, p. 233.

(6) Jain, V.K. and Pandey, P.C., Journal of Engineering for Industry, Trans ASME, MAY, 1931, Vol. 103/183.

(7) Chardasekar, N.S., " Electrochemical Machining With Programme Controlled Composite Tools", M. Tech. Thesis, I.I.T., Kanpur, July 1983.

(8) Raghuram V., Banerji, D. and Amitabha Ghosh, Proc. XI AIMTDR, IIT Madras-1984, p. 327.

(9) McGeough, J.A., Principles of Electrochemical Machining John Wiley and Sons Inc. N.Y. (1974).

(10) Debarr, A.E. and Oliver, D.A., Electrochemical Machining, American Elsevier Pub. Co. (1968).

(11) Amitabha Bhattacharya, New Technology, Institution of Engineers, Calcutta (1977).

(12) Smith, G.D., Numerical Solution of Partial Differential Equation, Ch.5, p. 153, 2nd ed., Oxford Clarendon (1973).

APPENDIX-A

The Laplace's equation in two dimensional cylindrical coordinates is as follows:

$$\frac{\partial^2 \phi}{\partial r^2} + \frac{\partial^2 \phi}{\partial z^2} + \frac{1}{r}\frac{\partial \phi}{\partial r} = 0 \qquad (1)$$

where $\phi = \phi(r, z)$

corresponding finite difference equation is

$$\frac{\delta^2 \phi}{\delta r^2} + \frac{\delta^2 \phi}{\delta z^2} + \frac{1}{r}\frac{\delta \phi}{\delta r} = 0 \qquad (2)$$

but $$\frac{\delta \phi}{\delta r} = \frac{\phi(i+1, j) - \phi(i, j)}{a} \qquad (3)$$

where $\phi(i, j)$ is the potential at any point (i, j)

a is a side of square mesh

$$\frac{\delta^2 \phi}{\delta r^2} = \frac{\dfrac{\phi(i+1, j) - \phi(i, j)}{a} - \dfrac{\phi(i, j) - \phi(i-1, j)}{a}}{a}$$

$$\frac{\delta^2 \phi}{\delta r^2} = \frac{\phi(i+1, j) - 2\phi(i, j) + \phi(i-1, j)}{a^2} \qquad (4)$$

similarly $$\frac{\partial^2 \phi}{\partial z^2} = \frac{\phi(i, j+1) - 2\phi(i, j) + \phi(i, j-1)}{a^2} \qquad (5)$$

Taking axisymmetry $r = ia$ and $z = a$

$$\frac{1}{r}\frac{\delta \phi}{\delta r} = \frac{1}{ia}\,\frac{\phi(i+1, j) - \phi(i-1, j)}{2a} \qquad (6)$$

substituting (4) (5) and (6) in equation (2), it becomes

$$\frac{\phi(i+1,j) - 2\phi(i,j) + \phi(i-1,j)}{a^2}$$

$$+ \frac{\phi(i, j+1) - 2\phi(i,j) + \phi(i,j-1)}{a^2}$$

$$+ \frac{1}{ia} \frac{\phi(i+1, j) - \phi(i-1,j)}{2a} = 0$$

Simplifying above equation we get,

$$\phi(i+1, j)\left(1 + \frac{1}{2i}\right) + \phi(i-1,j)\left(1 - \frac{1}{2i}\right)$$

$$+ \phi(i, j+1) + \phi(i, j-1) - 4\phi(i,j) = 0$$

Therefore

$$\left[\phi(i+1, j)\left(1 + \frac{1}{2i}\right) + \phi(i-1, j)\left(1 - \frac{1}{2i}\right)\right.$$

$$\left. + \phi(i, j+1) + \phi(i,j-1)\right]/4 = \phi(i,j)$$

APPENDIX-B

The Laplace's equation in three dimensional cartesian coordinates is as follows:

$$\frac{\partial^2 \phi}{\partial x^2} + \frac{\partial^2 \phi}{\partial y^2} + \frac{\partial^2 \phi}{\partial z^2} = 0 \qquad (1)$$

where $\phi = \phi(x,y,z)$

corresponding finite difference equation

$$\frac{\delta^2 \phi}{\delta x^2} + \frac{\delta^2 \phi}{\delta y^2} + \frac{\delta^2 \phi}{\delta z^2} = 0 \qquad (2)$$

but $$\frac{\phi}{x} = \frac{\phi(i+1, j, k) - \phi(i,j,k)}{a} \qquad (3)$$

where $\phi(i,j,k)$ is potential at any point (i,j,k)

a is a side of cubical mesh

$$\frac{\delta^2 \phi}{\delta x^2} = \left[\frac{\phi(i+1, j, k) - \phi(i,j,k)}{a} - \frac{\phi(i,j,k) - \phi(i-1,j,k)}{a} \right] / a$$

$$\frac{\delta^2 \phi}{\delta x^2} = \frac{\phi(i+1, j,k) - 2\phi(i,j,k) + \phi(i-1,j,k)}{a^2} \qquad (4)$$

similarly

$$\frac{\delta^2 \phi}{\delta y^2} = \frac{\phi(i,j+1,k) - 2\phi(i,j,k) + \phi(i,j-1,k)}{a^2} \qquad (5)$$

$$\frac{\delta^2 \phi}{\delta z^2} = \frac{\phi(i,j,k+1) - 2\phi(i,j,k) + \phi(i,j,k-1)}{a^2} \qquad (6)$$

substituting the equations (4), (5) and (6) in eq. (2) we get;

$$\frac{\phi(i+1,j,k) - 2\phi(i,j,k) + \phi(i-1,j,k)}{a^2}$$

$$+ \frac{\phi(i,j+1,k) - 2\phi(i,j,k) + \phi(i,j-1,k)}{a^2}$$

$$+ \frac{\phi(i,j,k+1) - 2\phi(i,j,k) + \phi(i,j,k-1)}{a^2} = 0$$

Therefore

$$[\phi(i+1,j,k) + \phi(i-1,j,k) + \phi(i,j+1,k)$$

$$+ \phi(i,j-1,k) + \phi(i,j,k+1) + \phi(i,j,k-1)]/6$$

$$= \phi(i,j,k)$$

A 87450

Thesis
621.93
B223a

DATE SLIP A87450

This book is to be returned on the date last stamped.

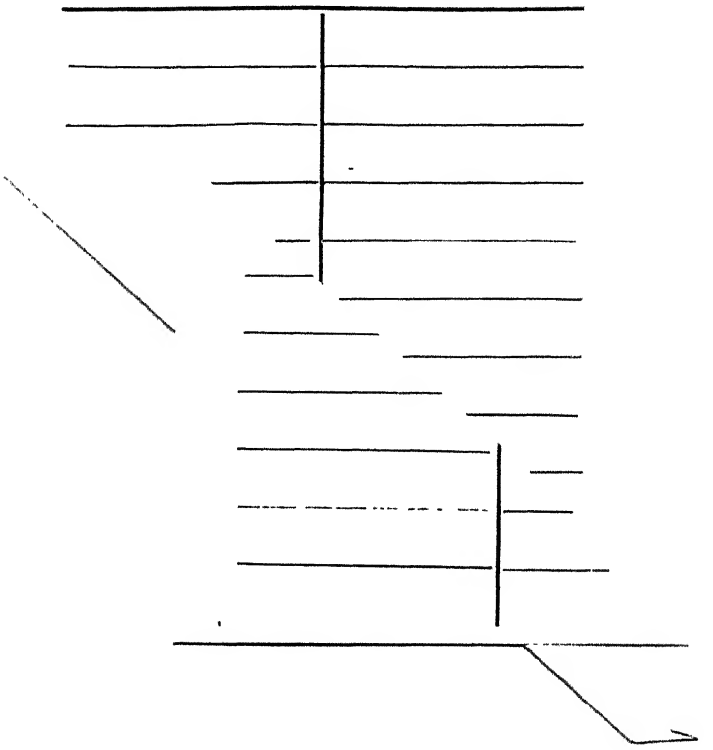

ME-1985-M-BAN-ANO

Thesis
621.93
B223a

A87450